Anatomical, Physiological, Molecular and Circuit Properties of Nest Basket Cells in the Developing Somatosensory Cortex

Yun Wang[1]*, Anirudh Gupta[2]*, Maria Toledo-Rodriguez[2], Cai Zhi Wu[2] and Henry Markram[2]

[1]Section of Neurobiology, Yale University School of Medicine, New Haven, CT 06520-8001, USA and [2]Department of Neurobiology, Weizmann Institute of Science, 76100 Rehovot, Israel

*Both authors contributed equally to the work presented in this manuscript

Anatomical, electrophysiological and molecular diversity of basket cell-like interneurons in layers II–IV of rat somatosensory cortex were studied using patch-clamp electrodes filled with biocytin. This multiparametric study shows that neocortical basket cells (BCs) are composed of three distinct subclasses: classical large (LBC) and small (SBC) basket cells and a third subclass, the nest basket cell (NBC). Anatomically, NBCs were distinct from LBCs and SBCs in that they formed simpler dendritic arbors and an axonal plexus of intermediate density, composed of a few long, smooth axonal branches. Electrophysiologically, NBCs exhibited diverse discharge responses to depolarizing current injections including accommodation, non-accommodation and stuttering. Single-cell multiplex RT-PCR revealed distinct mRNA expression patterns for the calcium binding proteins parvalbumin (PV), calbindin (CB) and calretinin (CR), and the neuropeptides somatostatin (SOM), vasoactive intestinal peptide (VIP), cholecystokinin (CCK) and neuropeptide Y (NPY) for each BC-subclass. SBCs lacked NPY expression but invariably expressed VIP, whereas neither VIP, CR nor SOM expression was detected in LBCs, and VIP and CR expression was absent in NBCs. Electrophysiologically distinct types of NBCs formed GABAergic synapses with specific dynamics onto pyramidal cells (PCs) and received either strongly facilitating or depressing synaptic inputs from PCs. Finally, NBCs were found to be the most common basket cell in layers II/III, while LBCs were the most common in layer IV. These data provide multiparametric distinguishing features of three major subclasses of basket cells and indicate that NBCs are powerful interneurons that provide most of the (peri-)somatic inhibition in the supragranular layers.

Introduction

GABAergic interneurons constitute only a minor fraction of the total number of neurons in the neocortex (15–25%) (Fairen *et al*., 1984; Houser *et al*., 1984; Peters, 1984), but are crucial for normal brain function (Berman *et al*., 1992; McBain and Fisahn, 2001). Despite their small numbers, these interneurons are extremely diverse in their morphological, electrophysiological and molecular properties (Fairen *et al*., 1984; White, 1989; DeFelipe, 1993; Cauli *et al*., 1997; Kawaguchi and Kubota, 1997; Gupta *et al*., 2000). However, the extent and functional significance of this diversity is not fully understood. Different types of interneurons could be specialized to exert specific effects on dendritic processing, summation of synaptic potentials or action potential (AP) discharge (Cobb *et al*., 1995; Miles *et al*., 1996; Larkum *et al*., 1999). Basket cells (BCs) were first described by Ramon y Cajal (Ramon y Cajal, 1911) according to their distinct axonal arborizations on and around somata of target neurons. Interneurons that form a high fraction of axo-somatic synapses have therefore traditionally been classified as BCs (Somogyi *et al*., 1983; Jones and Hendry, 1984). The strategic innervation of somata and proximal dendrites enables BCs to effectively control the gain of summated synaptic potentials and thereby the AP-discharge of target cells (Cobb *et al*., 1995; Miles *et al*., 1996). Basket cells are, however, diverse in terms of morphological properties (Fairen *et al*., 1984; Jones and Hendry, 1984; Peters and Saint Marie, 1984; Kisvarday, 1992; White, 1989; Gupta *et al*., 2000), immunoreactivities for different calcium binding proteins and neuropeptides (DeFelipe, 1993; Kawaguchi and Kubota, 1998), bouton ultrastructure (Peters and Harriman, 1992), electrophysiology (Thomson *et al*., 1996; Kawaguchi and Kubota, 1997; Dantzker and Callaway, 2000; Gupta *et al*., 2000), input specificity (Dantzker and Callaway, 2000; Krimer and Goldman-Rakic, 2001) and receptive field properties (Martin *et al*., 1983). Neither the functional significance nor the organizational principles underlying this diversity are known.

Two unambiguous subclasses of BCs are the classical large basket cells (LBCs) and small basket cells (SBCs). In the neocortex, LBCs are generally large, aspiny multipolar neurons that place ~20–40% of their synapses on target cell somata (Somogyi *et al*., 1983; Kisvarday, 1992). Their axons usually originate from the pial aspect of the soma, and typically ascend to give rise to many long horizontally and vertically projecting axon collaterals that traverse neighboring columns (generic ~300 μm diameter columns are used in this study to refer to the local microcircuitry) and can extend through all cortical layers. Smaller side branches terminate in pericellular baskets around somata and proximal dendrites of neurons (Somogyi *et al*., 1983; Jones and Hendry, 1984; Kisvarday, 1992). SBCs are also aspiny multipolar cells that place 20–30% of their synapses on target cell somata (Fairen *et al*., 1984; Kisvarday *et al*., 1985). Their axonal arbors, composed of frequent short, curvy axonal branches, tend to be near their somata and within the same layer. Multipolar neurons with radiating axonal collaterals that are not typical of either the LBC or SBC morphologies have been noted in passing by several authors (Jones, 1975; Feldman and Peters, 1978; DeFelipe and Fairen, 1982; Peters and Saint Marie, 1984; Lund and Lewis, 1993). These 'atypical' cells were identified as BCs because they targeted somata in synaptically coupled pairs, but were considered a separate class of basket cell because some morphological features differed from LBCs and SBCs, which led to the name 'nest basket cell' (Gupta *et al*., 2000).

In the present study, we focused on multiparametric features of a large number of BCs in order to examine the major subclasses of BCs, establish subjective and objective criteria to identify the different subclasses, determine their relative prevalence in this neocortical region, and explore how NBCs are integrated into the neocortical microcircuitry.

Whole-cell patch-clamp recordings of single and synaptically coupled interneurons in layers II–IV of rat somatosensory cortex were obtained. Recorded cells were filled with biocytin, histochemically stained and 3-D computer-reconstructed for morphometric analysis. Cytoplasm of some single cells was aspirated for subsequent multiplex RT-PCR in order to assess the expression profile of mRNAs for selected calcium binding proteins and neuropeptides. Electron microscopic (EM) examination of some

single cells and pairs of cells was also carried out in order to determine the location and distribution of synapses formed onto target neurons and to verify putative contacts of synaptically connected cells.

This study indicates that BCs are composed of three major subclasses and provides quantitative multiparametric data, which demonstrate that NBCs indeed comprise a distinct subclass of basket cell. The properties of local glutamatergic synapses received from neighboring PCs suggest that multiple PCs are required to recruit NBCs ('high threshold interneurons') while the properties of the GABAergic synapses formed by NBCs suggest that these interneurons can powerfully inhibit their targets. The high prevalence of NBCs, further indicate that these cells are a major source of (peri-) somatic inhibition in the supragranular and granular layers of rat neocortex.

Materials and Methods

Electrophysiology and Histology

Recording and staining procedures were as described previously (Markram *et al*., 1997). Briefly, Wistar rats (13–15 days) were rapidly decapitated and neocortical slices (sagittal, 300 μm thick) were sectioned (DSK, Microslicer, Japan) and recorded at ~32–34°C. Neurons in somatosensory cortex were identified using infrared differential contrast videomicroscopy (Zeiss – Axioplan, fitted with a 40×-W/0.75 NA objective; Zeiss, Oberkochen, Germany) and patch-clamp recordings obtained with biocytin-loaded (0.2%) pipettes that contained (in mM): 100 potassium gluconate, 20 KCl, 4 ATP-Mg, 10 phosphocreatine, 0.3 GTP, 10 HEPES (pH 7.3, 310 mosmol/l, adjusted with sucrose). Membrane and synaptic reversal potentials were not corrected for the junction potential between bath and pipette solutions (~ 9mV). The recorded neurons were selected up to 120 μm below the surface of the slice and separated from each other by up to 150 μm. After recording, slices were fixed with 2% paraformaldehyde, 1% glutaraldehyde and 0.3% saturated picric acid in 0.1 M phosphate buffer (pH 7.4), and subsequently visualized by the avidin–biotinylated horseradish peroxidase method with diaminobenzidine as chromogen (ABC-solution; ABC-Elite, Vector Labs, Peterborough, UK). Slices prepared for light microscopic examination were mounted directly onto slides with aqueous mounting medium. In some cases, slices were resectioned into 100 μm thick sections before mounting. Staining of slices for EM examination was modified based on the method of Han *et al*. (Han *et al*., 1993). Briefly, after the histochemical staining, the slices in which the filled cells were clearly visualized were resectioned at 60–80 μm thickness. Sections were post-fixed with 1% O_SO_4, block-stained in 1% uranyl acetate and dehydrated. After flat embedding into resin (Durcupan, Fluka, Buchs, Switzerland), light microscopic (LM) observation and 3-D reconstruction of the cells were carried out. Later some areas with rich interneuron boutons or putative synapses were re-embedded for cutting serial ultrathin sections, which were finally examined with EM.

Analysis of Electrophysiological Recordings

Most signals were sampled at 4 KHz (except for single action potentials and high-resolution unitary synaptic recordings, which were sampled at up to 20 KHz) and low-pass pre-filtered (4–8 pole Bessel).

Intrinsic Properties

Input resistances were approximated by linear regression of voltage deflections (±15 mV from resting potential, –75 ± 2mV) in response to 1 s current steps of 4–8 different amplitudes after reaching steady state (last 200 ms of a 1 s current pulse). Steady-state current–voltage relationships are sufficiently linear for most interneurons to allow this analysis. Membrane time constants were determined by fitting a monoexponential to the decay phases of depolarizing and hyperpolarizing delta-pulses (1 ms duration; voltage deflections of <10 mV), or from fitting a monoexponential to the rising phases of the voltage traces used for determining the input resistances. Single AP analysis was performed on the first AP elicited by threshold depolarizations. Peak values of the AP and the fast afterhyperpolarizations (fAHPs) were determined by averaging 3–5 values around the peak. Maximum rise and fall rates were obtained as peak values after differentiating the single APs. Discharge behaviors were classified according to Gupta *et al*. (Gupta *et al*., 2000). Somatic current injections causing discharges ranged from 30 to 600 pA, dependent on the cellular input resistance. Discharge behaviors were robust up to 4× threshold current injections (ranging from 45 to 280 pA). and stable for different holding potentials (from –85 to –60mV) and different temperatures (~20–24 and ~32–34°C). Various components of internal solutions may affect receptor functions and alter specific ionic conductances to amplify or attenuate electrophysiological differences. The standardized conditions in this study must therefore be considered when comparing these data with others.

Synaptic Properties

Whole-cell recordings typically result in low-noise recordings. The root mean square (r.m.s.) of the noise was measured 30–60 ms prior to the onset of the evoked postsynaptic potentials/currents (PSP/PSCs) of connected cells. Failures were defined as events in which the amplitude was less than the r.m.s. The latency of PSP/PSC onset was defined as the time from the peak of the AP to 10% of the PSP/PSC amplitude. This measure therefore includes axonal, synaptic and dendritic delays. PSP/PSC amplitudes were determined by averaging 3–5 points around the peak (not corrected for the CV of noise). Series resistance and whole-cell capacitance of voltage clamp recordings were in most cases (>80%) compensated by >85%. Rise times of currents (RT) were measured as time to rise from 20 to 80% peak amplitude (30–50 sweeps excluding failures). Decay time constants (DTC) of PSCs were estimated as single exponentials because of multiple distributed release sites. Chord conductances (G_1) were determined as the slope of the line fit through amplitudes of first responses and intersection at the reversal potential (negligible rectification detected). Maximal conductances (G_{max}) were calculated as G_1/Use (utilization of synaptic efficacy, equivalent to probability of release). Charge was determined by integrating the mean unitary inhibitory PSC (30–50 waves) excluding failures. Quantification of the physiological properties of unitary excitatory PSCs was not performed due to variable degrees of synaptic rundown (Rozov *et al*., 1998). Parameters of synaptic connections (Ase, absolute synaptic efficacy; Use; F and D, time constants for recovery from facilitation and depression, respectively) were derived by fitting averaged synaptic responses (30–60 trials) to at least two different frequencies of presynaptic stimulation to the model of dynamic synaptic transmission as detailed previously (Markram *et al*., 1998).

Three-dimensional Computer Reconstruction

Three-dimensional neuron models were reconstructed from stained cells using the Neurolucida system (MicroBrightField Inc., Colchester, VT, USA) and a brightfield light microscope (Olympus, Düsseldorf, Germany). Each neuron in a connection was reconstructed, and every location of putative synapses was marked on axonal and dendritic structures, as well as on somata with different markers. Putative synapses were identified according to the following criteria: (i) only contacts formed by axonal swellings (boutons) were considered; (ii) the same plane of focus (microscope lens with ×60 magnification, numerical aperture = 0.9; resolution along the *Z*-axis = 0.37 μm) was used. This requires bouton and somatic/dendritic/axonal to be membranes within <0.5 μm of each other; (iii) if the dendrite was thick (>2 μm) with many spines, then a greater distance between the bouton and dendrite was allowed, providing that the course of the axon bent towards or ran parallel to the dendrite. After the staining procedure, there is ~25% shrinkage of the slice thickness and ~10% anisotropic shrinkage along the *X*- and *Y*-axes. Only shrinkage of thickness was corrected.

Quantitative Morphometry

Reconstructed neurons were quantitatively analyzed with NeuroExplorer (Version 3.06, MicroBrightField Inc.) within the Neurolucida system. An array of eight axonal and six dendritic parameters, designated as the 'morphology code' (m-code), was obtained to quantitatively compare the axonal and dendritic arbors of the basket cell subclasses. The axonal parameters were as follows. (1) Axonal Sholl distance (ASD) was defined as the number of axonal intersections as a function of distance from the soma. A series of Sholl circles with 20 μm stepped radii centered

in the interneuron soma were delineated and the number of axonal intersections in each stepped region and their distances to the center were calculated (Sholl, 1956; Valverde, 1971). The maximum radius of Sholl circles used for the ASD-calculation was 1 mm. (2) Axonal segment lengths (ASL) are defined as the length of axonal segments between two branch points or between a branch point and an end point. (3) Axonal branch order (ABO) is the branching frequency of an interneuron axon tree. (4) Bouton density (BD) is calculated as the number of boutons per axon length. (5) Maximum axonal branch angle (MABA) denotes the maximum angle formed between the extending distal line of the parent axonal segment and child axonal segments. (6) Planar axonal branching angle (PABA) denotes the angle formed between the extending distal line of the parent axonal segment and a child axonal segment. (7) Total number of axonal segments (SEG). (8) Total number of boutons per cell (BT). Dendritic parameters were obtained by applying the same criteria as for the axonal structure and designated (1): dendritic Sholl distance (DSD); (2) dendritic segment length (DSL); (3) dendritic branch order (DBO); (4) maximum dendritic branch angle (MDBA); and (5) planar dendritic branch angle (PDBA), respectively. In addition, (6) the average length of dendritic tree (ALDT) was defined as the average length of a single dendrite including all its branches (dendritic tree). For some cells, the full m-code (14 parameter range) could not be obtained. These cases were excluded from the Fisher's linear discriminant analysis (see below).

For each class of connection, the pre- and postsynaptic innervation patterns were obtained according to the synapse distribution on the axonal and dendritic trees of the connected neurons. The parameters used for the quantitative analysis include: geometric and electrotonic distances, as defined previously (Markram *et al*., 1998); the innervated dendritic fraction, which refers to the fraction of the dendritic trees of the postsynaptic cell receiving contacts from the presynaptic cell; the innervating axonal fraction, which denotes the fraction of the primary axonal collaterals (PAC) utilized to innervate the postsynaptic neuron [a PAC denotes an axonal collateral (with all its sequential branches) emerging *directly* from the axonal main stem]; and the number of closely located putative synapses defined according to the distance between two putative synapses (proximity < 10 μm). Slice underestimates of the number of putative synapses are based on estimated loss of the dendritic field as a function of the arbor dimensions and the depth of the recorded cell in the slice.

EM Examination

In order to determine the postsynaptic targets of a filled interneuron, a region containing boutons only belonging to the studied interneuron was randomly selected. The targets of all the boutons encountered in subsequent serial sections were examined under EM according to established criteria (Peters *et al*., 1991). Briefly, a postsynaptic target of a filled bouton was judged to belong to soma/dendrite/spine based on its ultrastructural characteristics. Identification of the nature of postsynaptic dendritic shafts (pyramidal versus interneuron) was done according to previous studies (Hornung and Garey, 1981; Kisvarday *et al*., 1985; Peters *et al*., 1991). Synapses formed between connected neurons were examined at the EM level according to a widening synaptic cleft formed between rigid pre- and postsynaptic membranes and vesicle accumulation in the presynaptic bouton (when the presence of peroxidase reaction product was not too dark) (Tamas *et al*., 1997b). When the plane of the section was not perpendicular to the junction of membranes, the synaptic cleft was recognized by tilting the section using the goniometer of the EM. Eighty-three percent of LM identified synapses were EM verified (10/12 putative synapses).

Single-cell Reverse Transcriptase (RT) Polymerase Chain Reaction (PCR)

At the end of the recording, cell cytoplasm was aspirated into the recording pipette under visual control by applying gentle negative pressure. Only cells in which the seal was intact throughout the recording and during the aspiration were further processed. Reverse transcription was performed using an oligo-dT primer and 100 units of MMLV reverse transcriptase (Gibco, BRL) (Lambolez *et al*., 1992). After 50 min incubation at 42°C, the cDNA was frozen and stored at –20°C before further processing. Subsequently, multiplex PCR was carried out (Cauli *et al*., 1997), allowing simultaneous amplification of mRNA transcripts for the calcium binding proteins (CB, PV and CR), the neuropeptides (NPY, VIP, SOM and CCK) and GAPDH (used as a positive control for the harvesting procedure). The primers used for the PCR are described by Cauli *et al*. (Cauli *et al*., 1997), while those used for GADPH are described by Aranda-Abreu *et al*. (Aranda-Abreu *et al*., 1999). Amplification specificity was verified by restriction analysis. Controls for possible contamination artifacts were performed for each PCR amplification. Amplification of genomic DNA was excluded by the intron-overspanning primers and by not harvesting the nucleus. The PCR study was performed on a separate population of single cells, recorded at room temperature and therefore excluded from single AP waveform analysis.

Statistical Analysis

Unpaired Student's *t*-tests were applied to compare between the means of groups. Unpaired non-parametric tests (Mann–Whitney) were employed to compare the medians of two groups with sample sizes of <8. Chi-square (χ^2) tests were applied to compare two distributions. In order to determine the significance of the proposed subclassification of BCs, we carried out Fisher's linear discriminant analysis (Fukunaga, 1990). Separability values (represented as discriminant scores, DS) for points where each point is a cell in a 14-dimensional parameter space (m-code of 14 morphological features) were calculated as the ratio between the inter-class and intra-class spread. The result of the calculated separation is visualized by projecting the points onto an optimal hyperplane (described by the coefficients C1 and C2), reflecting the value of the DS and the quality of the separation. In order to test the validity of the proposed subclassification, the labels of the data points were randomly scrambled (i.e. their assignments to the three morphological subclasses) and the Fisher analysis was repeated 10 000 times. In 9520 cases the random partition yielded DS < 23.98, which was the score for the proposed subclassification. The probability of mistakenly identifying three groups in this data set is therefore $P < 0.048$.

Results

Large, Small and Nest Basket Cells

One hundred and forty-six anatomically verified basket cell-like interneurons were examined throughout layers II–IV (LII/III, $n = 93$; LIV, $n = 53$), including 27 SBCs, 47 LBCs and 72 NBCs (Fig. 1). Discharge properties for 79 of these cells (12 SBCs, 26 LBCs and 41 NBCs) were analyzed in detail. Of these neurons, 37 were 3-D computer-reconstructed (10 SBCs, 10 LBCs and 17 NBCs; Table 1) from which 21 yielded a complete 14 parameter morphological profile. Twenty-six of the 79 cells were analyzed for their detailed electrophysiological properties (passive properties and single AP analysis; Table 1), and single-cell RT-PCR was performed for 66 of the 146 cells (18 SBCs, 19 LBCs and 29 NBCs; Table 1).

Axonal and dendritic morphologies of many basket cell-like interneurons exhibited patterns typical of SBCs and LBCs (Fig. 1), but most cells actually differed from these classical patterns. The axon collaterals of these atypical cells lacked soma-targeting signs that usually guide light microscopic studies to conclude that interneurons are putative BCs, but reconstructions of synaptically coupled pairs revealed putative synapses onto and close to somata of target cells. In some cases, their axonal arbor appeared to be more similar to SBCs in that they formed a rather dense local plexus around their soma, but a quantitative analysis revealed much fewer axonal segments making up the plexus (Table 1). In other cases, they appeared similar to LBCs in that they formed a sparse local plexus with some farther-reaching axonal collaterals, but these collaterals differed from those of LBCs in that they were smoother, with fewer side branches. In yet further cases, they appeared to share features of both SBCs and LBCs.

To examine whether these cells are *de facto* BCs according to established criteria (Jones and Hendry, 1984; Freund *et al*., 1986;

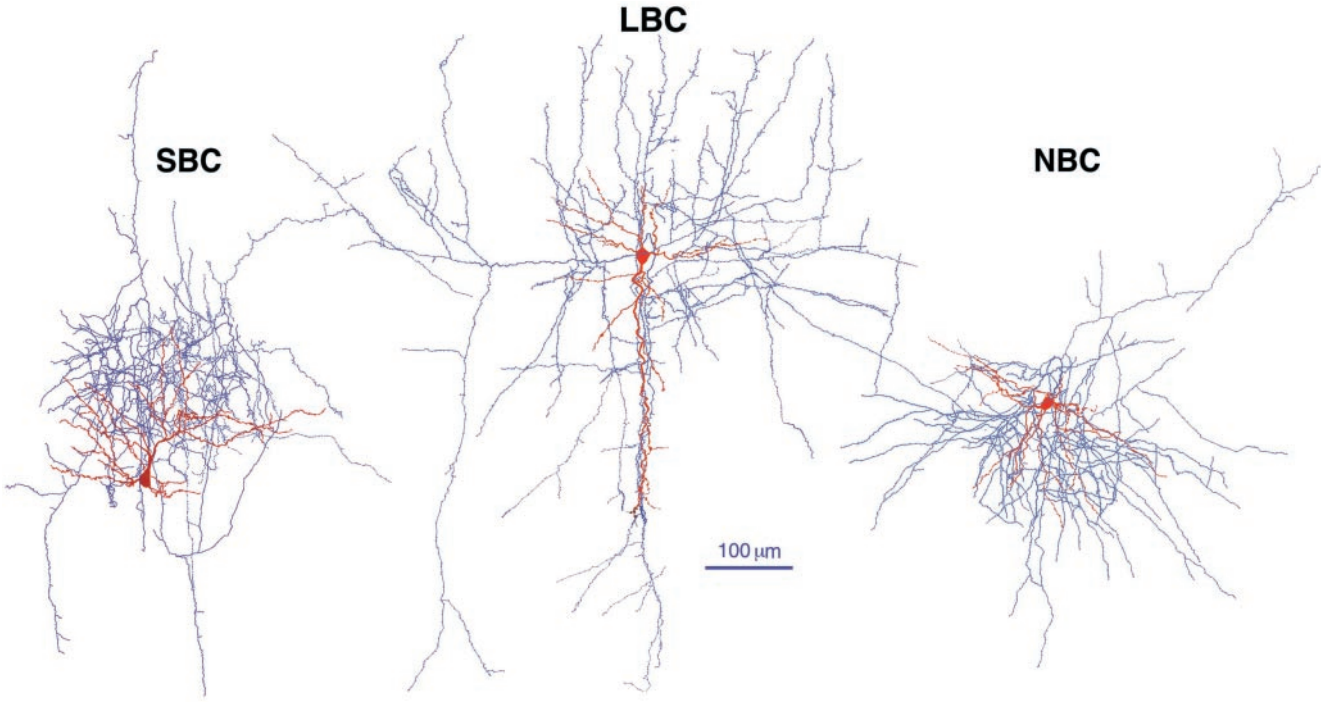

Figure 1. Three subclasses of neocortical basket cells. Three-dimensional computer reconstructions of an SBC, an LBC and an NBC, all located in layer IV. Somata and dendrites, red; axons, blue. SBC axonal arbor with frequently branching, short, curvy axonal segments densely studded with boutons. LBC axonal arbor with few axonal segments and long vertical and horizontal axonal collaterals. NBCs axonal arbor with a local axonal cluster consisting of long smooth segments studded with few boutons. The dendritic structure of NBCs is less complex than both SBCs and LBCs.

Somogyi and Soltesz, 1986; Kisvarday, 1992), the synaptic targets of these interneurons were examined at the EM level. We only succeeded in obtaining high quality EM for four NBCs, because the ultrastructural quality is very sensitive to a number of factors (duration of recording, cell conditions and health after recording, fixing, staining and further processing procedures). Eighty-three synaptic junctions were identified at 74 randomly selected boutons from these four cells (1.1 synapses/bouton). As for LBCs and SBCs (data not shown), symmetrical synapses formed by NBCs were located on postsynaptic somata [range, 14–47%; mean, 23%; median, 16%; Fig. 2*a*; see also (Kisvarday, 1992)]. In addition, synapses were formed onto dendritic shafts (59%; Fig. 2*b*,*c*) and spines (18%; Fig. 2*d*). This synaptic distribution and the high fraction of axo-somatic synapses is characteristic of BCs (Kisvarday, 1992), indicating that these atypical cells are indeed BCs. The local axonal cluster of these neurons resembles a messy bird's nest, and they were hence named 'nest basket cells' (Gupta *et al.*, 2000).

In order to quantitatively compare SBCs, LBCs and NBCs, an array of morphological properties was analyzed (Table 1). The axonal morphology is generally more characteristic of the interneuron type (Jones, 1975; Fairen *et al.*, 1984; White, 1989; Lund and Lewis, 1993). Three parameters were particularly informative (see Materials and Methods): (i) ASD (Sholl, 1956; Valverde, 1971); (ii) ASL; and (iii) ABO. Each of these parameters describes a specific feature of the local axonal plexus: ASD reflects its spread, and ASL and ABO reflect length and order of axonal segments forming the plexus, respectively. The ASD values of NBCs were similar to those of SBCs, but significantly smaller than those of LBCs (χ^2, $P < 0.01$) as expected from the presence of their local axonal plexus. The axonal plexus of NBCs, however, differed from that of SBCs in that the segments making up the plexus were much fewer and significantly longer (χ^2, $P < 0.01$; see also Table 1). The NBC axons also did not branch as profusely as SBC axons and, therefore, produced a local plexus that is made up mostly of low order branches (Table 1). Indeed, whereas SBCs produced up to 35th order axonal branches, NBCs only reached 19th order branching (LBCs up to 25th order). The axonal arbor of NBCs was furthermore studded with a lower density of boutons while the number of putative synapses formed by NBCs onto pyramidal neurons (see below) was not significantly different from those formed by SBCs, indicating that an individual NBC innervates less PCs than a SBC (Table 1). NBCs were also different in their dendritic structure, with simpler arbors than SBCs and LBCs, as manifested in lower DBOs and ALDTs (Table 1).

Purely objective classification schemes are not yet possible and our approach was therefore to ask whether our subjective pre-selection was valid. The quantitative analysis revealed that predefined LBCs, SBCs and NBCs were different in specific anatomical aspects, but in order to quantify overall morphological differences between these basket cell subtypes, we derived a morphology code (m-code) based on 14 axonal and dendritic parameters (normalized) (Fig. 3*a*) and tested whether these groups were significantly different. Fisher's linear discriminant analysis (Fukunaga, 1990) of those cells for which the complete m-code was derived ($n = 21$; see Materials and Methods) revealed that the discriminant score for separating SBCs, LBCs and NBCs (Fig. 3*b*) was higher than for 95% of 10 000 random groupings (Fig. 3*c*; $P < 4.8\%$; see Materials and Methods). While this is still not a blind test, it does indicate that it is valid to solve the practically relevant problem of pre-classifying BCs according to subjective criteria and supports the claim that these subclasses are morphologically distinct.

We further examined the extent to which these cells are electrophysiologically and molecularly different from each other.

Table 1
Comparison of anatomical, physiological and molecular properties of LBCs, NBCs and SBCs

	LBC	NBC			SBC
Anatomical properties	(n = 10)	(n = 17)			(n = 10)
Axonal					
ASD[a] (μm)	225 ± 11	165 ± 11*			145 ± 15
ASL (μm)	48 ± 3	50 ± 2**			32 ± 2
ABO	21 ± 4	17 ± 2*,**			23 ± 6
BD (boutons/μm)	0.184 ± 0.031	0.196 ± 0.034*			0.239 ± 0.045
SEG	365 ± 24	255 ± 23*,**			411 ± 173
BT	3165 ± 523	2481 ± 833*			3056 ± 1420
MABA (degrees)	67 ± 2	70 ± 2			73 ± 2
PABA (degree)	47 ± 1	57 ± 1*			52 ± 2
Dendritic					
DSD (μm)	99 ± 8	95 ± 7			104 ± 17
ASL (μm)	65 ± 5	63 ± 3			53 ± 3
DBO	4.0 ± 0.4	3.1 ± 0.2**			4.2 ± 0.5
ALDT (μm)	645 ± 109	397 ± 61*,**			619 ± 133
MDBA (degree)	56 ± 3	57 ± 1			54 ± 3
PDBA) (degree)	41 ± 2	41 ± 2			44 ± 3
Somatic					
% of basket cell–like interneuron located in L2/3 (n = 65)	23	73			4
% of basket cell–like interneuron located in L4 (n = 47)	46	34			20
Horizontal diameter (μm)	13.5 ± 3.6	13.5 ± 3.6			12.7 ± 1.8
Vertical diameter (μm)	23.2 ± 4.4	20.2 ± 2.4			20.7 ± 4.0
Physiological properties[b]					
Subclass according to discharge behavior	d–NAC (n = 5)	d–NAC (n = 5)	c–NAC (n = 5)	c–AC (n = 7)	c–AC (n = 4)
Passive properties					
Input resistance (MOhm)	121.61 ± 9.45	178.53 ± 57.82*	142.91 ± 54.34	174.03 ± 61.66	103.47 ± 23.32
Membrane time constant (ms)	14.04 ± 6.27	15.43 ± 5.13	14.74 ± 7.89	20.41 ± 8.25	14.78 ± 4.59
Single AP parameters					
AP_threshold (mV)	–34.9 ± 2.18	–34.7 ± 7.14	–41.41 ± 6.5	–39.9 ± 6.46	–43.05 ± 2.89
AP_amplitude (mV)	45.26 ± 9.09	39.96 ± 10.96	48.7 ± 15.3	47.92 ± 8.77**	61.43 ± 6.71
AP_half–duration (ms)	0.78 ± 0.08	1.16 ± 0.20***	1.02 ± 0.44	1.10 ± 0.23	1.14 ± 0.10
AP_chord rise rate (V/s)	80.57 ± 23.23	45.14 ± 19.74*	77.78 ± 42.20	58.72 ± 12.95**	82.68 ± 13.51
AP_maximum rise rate (V/s)	131.14 ± 45.36	79.55 ± 46.66	132.90 ± 64.46	106.81 ± 29.25	131.84 ± 28.36
AP_maximun fall rate (V/s)	–70.02 ± 17.47	–42.30 ± 14.25*	–68.62 ± 37.02	–61.62 ± 19.70	–55.99 ± 9.70
fAHP_amplitude (mV)	18.78 ± 0.39	17.18 ± 3.36	18.0 ± 5.3	14.84 ± 4.19	10.79 ± 2.93
Molecular properties	(n = 19)	(n = 29)			(n = 18)
Calcium binding proteins (%)					
PV	47	52			5
CB	26	34			16
CR	0	0			11
Neuropeptides (%)					
NPY	42	31			0
SOM	0	31			28
CCK	42	31			72
VIP	0	0			100
GAPDH	100	100			100

[a]Abbreviations are defined in the text.

[b]Comparisons performed for cells of same electrophysiological subclass, i.e. same discharge behaviours; see also (Gupta *et al*., 2000).

*Significantly different from that of LBC ($P < 0.05$).

**Significantly different from that of SBC ($P < 0.05$).

***Significantly different from that of LBC ($P < 0.01$).

Physiological properties were diverse within all three subclasses with overlapping discharge behaviors (Table 1, Fig. 4), although NBCs exhibited the greatest diversity, with as many as eight different subtypes of discharge responses (SBCs: four subtypes; LBCs: six subtypes). The input resistances of NBCs were generally higher compared to SBCs and LBCs with similar discharge behaviors, probably reflecting their simpler dendritic structures (Table 1). Some of the features of action potentials generated by NBCs also differed from those LBCs and SBCs that exhibited similar discharge patterns (Table 1).

To compare molecular properties of SBCs, LBCs and NBCs, single-cell RT-PCR was performed and mRNA expression patterns of different calcium binding proteins (PV, CB, CR) and neuropeptides (NPY, VIP, SOM, CCK) were obtained (Table 1) (DeFelipe, 1993; Cauli, *et al*., 1997; Kawaguchi and Kubota, 1997). NBCs, which may be mistaken for SBCs on cursory anatomical inspection, did not express mRNA for VIP (0/29 cases), while the mRNA for this neuropeptide was expressed by SBCs in all of the cases (18/18) (Kawaguchi and Kubota, 1996). SBCs, on the other hand, did not express mRNA for NPY (0/18), which was expressed by some NBCs (9/29). Furthermore, SBCs expressed mRNA for CCK (13/18) (Kubota and Kawaguchi, 1997) more commonly than NBCs (9/29). NBCs also differed in their expression profile from LBCs in that NBCs could express mRNA for SOM (9/29), which was not detected in LBCs (0/19). Even though false negatives may occur, it is unlikely that they

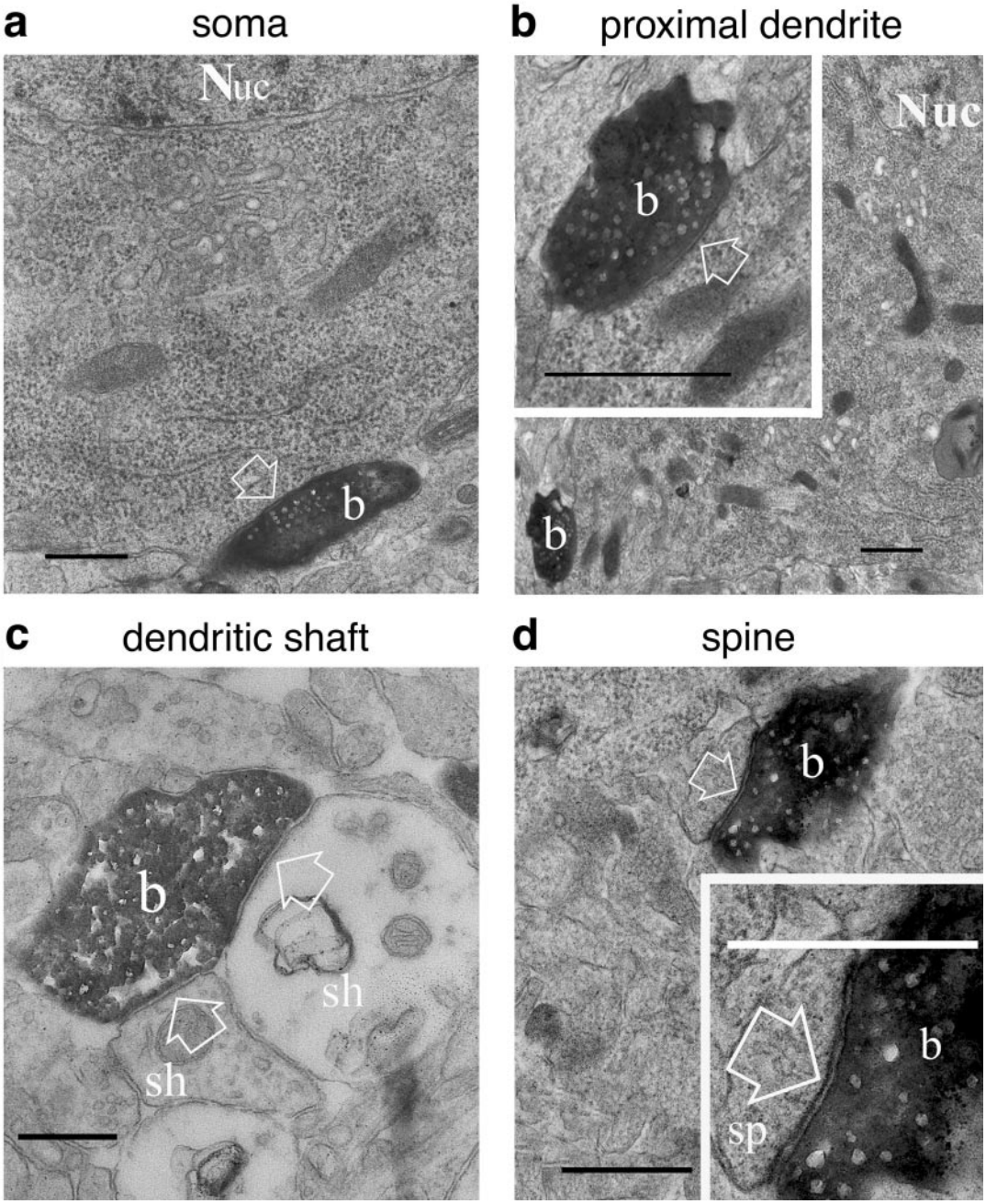

Figure 2. Random EM examination of NBC boutons: (*a*) Axo-somatic synapse. Note packaging of synaptic vesicles along the presynaptic membrane. (*b*) Axo-dendritic synapse. Inset depicts the synaptic cleft and the postsynaptic density after tilting the section using the goniometer of the electron microscope. This synapse was formed onto a dendritic main stem, where it emerged from the soma. Boutons in (*a*) and (*b*) are from same NBC. (*c*) Axo-dendritic shaft synapse. A single bouton simultaneously forming synaptic contacts onto the dendritic shafts of a presumed pyramidal cell (upper dendritic shaft with light cytoplasm) and a presumed interneuron (lower dendritic shaft with darker cytoplasm), respectively. (*d*) Axo-spinous synapse. Note rigid and parallel pre-postsynaptic membrane appositions outlining the synaptic cleft at higher magnification (inset). Nuc, nucleus; b, bouton; sh, dendritic shaft; sp, spine; arrow, synaptic junction; all scale bars = 0.5 μm.

would occur consistently in cells pre-selected on anatomical bases. These data therefore indicate that the three subclasses of BCs do not simply lie on a smooth continuum of molecular diversity and strongly support the anatomical and electrophysiological evidence that these cells constitute distinct basket cell subclasses. While mRNA expression patterns for calcium binding protein were less distinctive for the different subclasses of BCs, some trends seem to emerge; CR mRNA expression was detected only, albeit rarely (11%), in SBCs; PV mRNA was commonly expressed in LBCs (47%) and NBCs (52%), but expressed only rarely in SBCs (5%); mRNA for CB was expressed with low frequency in all three subclasses (26% of LBCs; 16% of SBCs; 34% of NBCs).

An analysis of the prevalence of interneuron types revealed that BCs comprise the major population (roughly 50%) of all the interneurons recorded in layers II/III (unpublished observation).

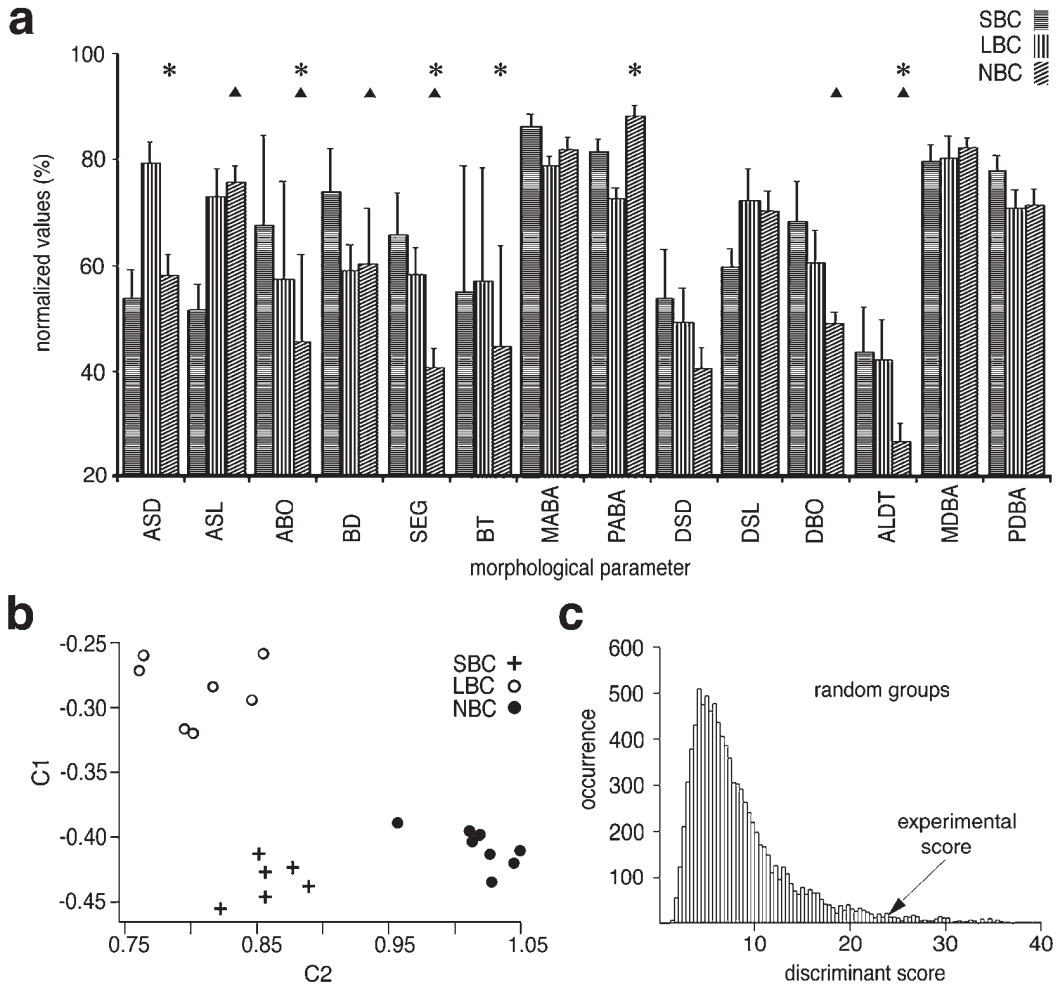

Figure 3. Morphological codes (m-codes) and Fisher's linear discriminant analyses demonstrate the distinctiveness of the three BC-subclasses. (*a*) Comparison of 14 morphological properties of SBCs ($n = 10$; horizontal hatching), LBCs ($n = 10$; vertical hatching) and NBCs ($n = 17$; cross-hatching). Values normalized to maximum values encountered for each parameter, and given as mean ± SEM, except for ABO, BD, SEG and BT (mean ± SD). NBCs differ significantly in seven axonal and two dendritic parameters from LBCs (asterices, $P < 0.05$) and/or from SBCs (filled triangles, $P < 0.05$). Graph includes also cells for which limited parameter sets were obtained (see Materials and Methods). (*b*) Fisher's L-class discriminant analysis was performed on cells, for which the full m-code [(all 14 parameters; see (*a*)] was obtained ($n = 21$), revealing the separation into three clusters. Axes denote constants C1 and C2 of the optimal hyperplane (see Materials and Methods). (*c*) Comparison of discriminant score of the proposed subclassification (arrow, experimental score = 23.98) to scores from 10 000 random partitions (see Materials and Methods). Only 4.8% of the random groups had a separability value higher than the proposed subjective classification (confidence level >95%).

Of the BCs, NBCs were the most common type encountered in layers II/III while LBCs were the most common in layer IV (Table 1).

Anatomical, Electrophysiological and Molecular Properties of NBCs

NBC somata were mostly irregularly shaped, giving rise to beaded and almost spine-free dendrites projecting in all directions (Table 2). Axons emerged more frequently from somata than from dendrites. During its course, the axonal main stem usually generates 5–6 PACs that sequentially arborize to form the characteristic local, loose nest-like plexus around the parental somata. Ultrastructural examination of randomly selected postsynaptic targets at the EM level revealed symmetrical synapses mostly onto pyramidal cells (~6:1; 86% of shaft synapses onto PCs, 14% onto interneurons; only synapses for identified targets counted; see Materials and Methods). With ~1.1 synapses/bouton, NBCs form a total of ~2800 synapses in slices (Table 1) and probably ~3700 *in vivo* (~25% average slice underestimation; see Materials and Methods). About 2/3 of the axonal tree of NBCs lie within 150 μm from the soma, indicating that most of the inhibition is applied in the local microcircuit (intracolumnar) and that a single NBC could contact 150–170 PCs (~16 synapses/ connection; see below).

Physiologically, these cells display diverse discharge responses to sustained somatic current injections (Fig. 4). According to a previous classification scheme based on discharge responses (Gupta *et al*., 2000), 61% displayed non-accommodation (NAC, Fig. 4*a*), 34% showed spike train accommodation (AC, Fig. 4*a*) and 5% were stuttering cells (STUT, Fig. 4*a*). Non-accommodating NBCs produced much stronger fAHPs than accommodating NBCs (Table 1). This type has been generally referred to as 'fast spiking' (Connors and Gutnick, 1990; Cauli *et al*., 1997; Kawaguchi and Kubota, 1997; Thomson and Deuchars, 1997). Cells belonging to each of the major categories (NAC, AC and STUT) were found throughout layers II–IV. Each of the major categories can be further subclassified according to the presence of transient delays (d-subclass), bursts (b-subclass) or their absence (designated as classical or c-subclass) before the characteristic discharges ensue, yielding eight subclasses of

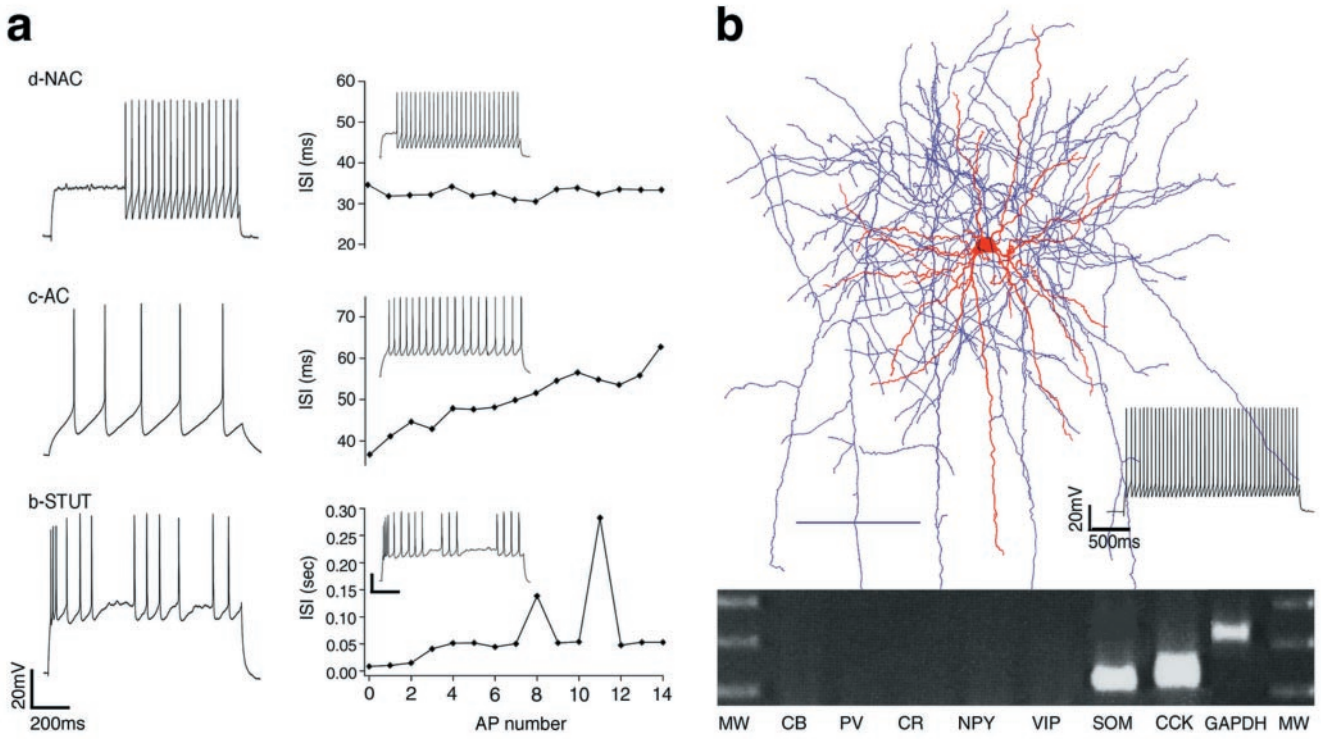

Figure 4. Electrophysiological and molecular diversity of NBCs. (*a*) Electrophysiological classification according to discharge responses to sustained somatic current injections. Non-accommodating (NAC) cells display virtually no change in inter-spike intervals (ISIs); accommodating (AC) cells show gradual increase in ISIs and stuttering (STUT) cells display abrupt jumps in ISIs. Further subclassification according to presence of a transient delay (d), burst (b) or absence of either delay/burst (classical, c). Inset scale bar: 20 mV, 200 ms. (*b*) Example of one of 29 anatomically 3-D reconstructed, electrophysiologically and molecularly characterized NBCs. This cell, a layer II/III c-NAC (see inset, bottom right), is one molecular subtype of NBC coexpressing mRNAs for SOM and CCK and lacking detectable levels of any calcium binding proteins. Soma and dendrites in red; axon in blue. Scale bar, 100 μm. MW, molecular weight marker.

NBCs (d-NAC, 46.4%; c-NAC, 12.2%; b-NAC, 2.4%; d-AC, 4.9%; c-AC, 19.5%; b-AC, 9.8%; c-STUT, 2.4%; b-STUT, 2.4%). NBCs discharging after a delay displayed a much higher AP-threshold than classically discharging NBCs (Table 1). It is not yet clear whether this electrophysiological diversity is correlated with anatomical heterogeneity within the NBC subclass.

Examination of the molecular properties of NBCs revealed diverse mRNA profiles. They typically coexpressed mRNAs encoding for 2–3 (maximum 5) molecular markers (Fig. 4*b*). mRNAs for calcium binding proteins (PV, 15/29; CB, 10/29; PV+CB, 8/29) and neuropeptides were coexpressed [SOM, 9/29; CCK, 9/29; NPY, 9/29; SOM+CCK, 4/29; SOM+NPY, 3/29; see also (Cauli *et al.*, 1997)]. Consistently, we found that NBCs frequently expressed mRNA for PV (15/29), sometimes in combination with other neuropeptides (PV+CCK, 3/29; PV+SOM, 3/29). The presence of PV is commonly associated with 'fast spiking' behavior (Cauli *et al.*, 1997; Kawaguchi and Kubota, 1997), a description that likely embraces different subclasses of NAC, AC and STUT cells. NBCs that expressed mRNA for CB were also found to coexpress mRNAs for some neuropeptides (CCK, 3/10; SOM, 3/10; NPY, 2/10). In none of the 29 cases studied did NBCs express mRNAs for CR or VIP.

Anatomical and Physiological Properties of Synaptic Innervation from NBCs onto PCs

Synaptic connections from 32 NBCs to pyramidal cells (PCs) were recorded throughout layers II–IV. Six of these connections were anatomically reconstructed (Fig. 5*a*). Ninety-three putative synapses were found at the LM level and quantitatively analyzed (Table 3). NBCs formed 15.8 ± 4.1 putative synapses onto postsynaptic PCs. Analysis of the detailed synaptic innervation pattern (see Fig. 5*b*) revealed 11% of synapses on PC somata. This is lower than the number of synapses estimated from the random EM examination (23% for all targets), probably reflecting a tendency to underestimate the number of axo-somatic contacts at the LM level (Tamas *et al.*, 1997a,b, 1998). This average fraction was, however, considerably higher than for dendritic-targeting interneuron types such as Martinotti, bitufted, double bouquet, neurogliaform and bipolar cells (unpublished data), and most of the remaining synapses were peri-somatic (see below). It is also not a fixed rule that BCs place synapses onto the somata of every single target cell (Somogyi *et al.*, 1983; Kisvarday *et al.*, 1987; Tamas *et al.*, 1998), which can result in lowering the average for synaptically coupled pairs. Indeed, out of six pairs of reconstructed connections, one pair did not form any axo-somatic synapses, but the synapses were peri-somatic and this interneuron displayed the characteristic axonal and dendritic morphologies of NBCs. Furthermore, in one pair (out of four connections) of a morphologically identified LBC onto a PC, and two pairs (out of seven connections) of SBCs contacting PCs, no putative synapses were found on the somata of the PCs. Similar results were also reported previously (Kisvarday *et al.*, 1987; Tamas *et al.*, 1998). A fixed percentage of somatic synapses in selected synaptically coupled pairs can therefore not be used as the sole criteria for identifying BCs. On the other hand, the peri-somatic nature of most synapses was consistent in all connections and could be quantified in terms of the average steady-state electrotonic distance for all synapses in the connection. The electrotonic distances of putative synapses from somata lay on a strongly skewed distribution, with >80%

Table 2
Anatomical properties of NBCs

Parameter	Result
Soma	
Location	L2/3: 76%; L4: 24%
Diameter (μm)	12.5 ± 1.6 (horizontal); 20.0 ± 2.5 (vertical)
Pericellular length (μm)	61.9 ± 6.9
Pericellular area (μm^2)	187.5 ± 36.4
Shape	irregular, 63.6%; triangle, 6.5%; round, 12.1%; ovoid, 15.2%; spindle, 3.2%
Dendrite	
No. of dendrites /cell	6.7 ± 2.0
Total dendritic length (μm)	2371.3 ± 890.2
ALDT (μm)	396.7 ± 61.1
Total dendritic surface area (μm^2)	4773.3 ± 1829.2
Total dendritic volume (μm^3)	986.3 ± 294.5
Maximum DBO	5.8 ± 1.4
Diameter of dendritic cluster (μm)	238.8 ± 47.5 (horizontal); 317.6 ± 91.3 (vertical)
Main long dendrite	no, 22 (67%); descending, 11 (33%)
Bitufted dendritic shape	no, 27 (82%); bitufted, 6 (18%)
Beaded[a]	most, 8 (24.2%); terminal, 11 (33.3%); common, 11 (33.3%); no, 3 (9.1%)
Spiny[b]	no, 9 (27.3%); a few, 11 (33.3%); sparsely, 11 (33.3%); middle, 2 (6.1%)
Axon[c]	
Axon origin	soma, 27 (66%); primary dendrite, 14 (34%)
Initial axonal direction	ascending, 30 (73.2%); descending, 8 (19.5%); one side, 3 (7.3%)
Total axonal length (μm)	12632.9 ± 3896.7
Total axonal volume (μm^3)[d]	1183.7 ± 420.1
Total axonal surface area (μm^2)[d]	15113.6 ± 5079.2
Maximal diameter of axon cluster (μm)	583.4 ± 255.1(horizontal); 643.9 ± 164.6 (vertical)
Diameter of local axon cluster (μm)	294.5 ± 87.2 (horizontal); 340.9 ± 127.2 (vertical)
Bouton density (BD) (bouton/μm)	0.196 ± 0.034

[a]Beaded: 'most': >3/4 segments; 'terminal': only terminal segments; 'common': between 'most' and 'terminal' grades; 'no': no beaded structure at all.

[b]Spiny: 'no': no spine at all; 'a few': occasionally spines encountered; 'sparsely': ≤3/10 μm;' middle': 4–10/10 μm; 'densely': >10/10 μm.

[c]Axonal parameters were obtained from a sample of 41 NBCs, whereas dendritic and somatic parameters include only 33 NBCs, due to incomplete dendritic staining.

[d]The total axonal volume and surface area of the axonal braid and boutons. At LM level, the average diameters of common and ultra-size boutons were 0.5 and 2 μm, respectively.

below 0.1λ (Table 3; maximal synapse distance, 0.3λ), indicating that the majority of synapses are either on or close to the soma.

Consistent with proximal synaptic locations, the mean latency of unitary responses following an AP in the NBC (reflecting axonal, synaptic and dendritic delays) was brief (0.91 ± 0.24 ms; Table 3). Axo-dendritic synapses were widely distributed across the dendritic domain of the postsynaptic PC (innervated dendritic fraction, 78%; Fig. 5*b*, Table 3), as were the boutons forming these synapses on the axonal domain of the presynaptic NBCs (innervating PAC fraction, 83%; Fig. 5*c*, Table 3). The large number of deployed synapses may increase reliability of transmission. Indeed, synaptic failure rates for these connections were negligible (Table 3).

The synaptic innervation pattern revealed that all dendritic compartments of PCs are potential targets for NBC innervation with ~1/3 of the axo-dendritic synapses located on apical dendrites and about 2/3 on basal dendrites (Fig. 5*b*). These fractions are approximately proportional to the relative length of respective dendrites. Dense innervation of PC apical dendrites is also found in connections from LBCs and has been suggested to be the optimal region to control inputs from several layers (Somogyi *et al.*, 1983). A high fraction of axo-dendritic synapses (43%) were located within 10 μm of each other, alluding to a tendency to form multiple synapses when the axon collateral approaches the dendrite.

Synaptic responses recorded from NBCs onto PCs were purely mediated by GABA-A receptors, as confirmed by their reversal potentials (Fig. 6*a*) and/or the characteristically slow decay time constants of their currents (Fig. 6*b*) (Galarreta and Hestrin, 1997). In some cases, bicuculline (a GABA-A receptor antagonist) was applied, causing complete and reversible blockade (Fig. 6*c*). GABAergic synapses are known to be different in terms of their dynamics of synaptic transmission. Three types of GABAergic synapses (termed F1-, F2- and F3-type synapse, respectively) were previously described according to the ratio of their underlying time constants of recovery from synaptic facilitation and depression (DF ratio) (Gupta *et al.*, 2000). Most (26/32) NBC to PC connections were of the F2-type (Fig. 6*d*), which characteristically show gradual depression of consecutive PSCs within a regularly spaced train for low frequencies (≤20 Hz; Fig. 6*d*), and transient facilitation during high frequencies (40–70 Hz; Fig. 6*d*). A characteristic feature of F2-type synapses is a depressed recovery test response (RTR, typically probed 500 ms after train) compared with the last response within the train (Fig. 6e). This behavior is due to synaptic depression outlasting facilitation several fold (~45-fold) (Table 3). Only 6/32 synaptic connections were of the F3-type, which exhibit a high capacity for sustained output due to rapid recovery from synaptic depression and facilitation (not shown). These synapses can be subjectively identified by a completely recovered RTR compared to the first response (Fig. 6f). Consistent with previously defined principles of GABAergic synaptic organization (Gupta *et al.*, 2000) different electrophysiological subtypes of NBCs formed distinct types of synapses onto PCs (Table 3).

Anatomical and Physiological Properties of Synaptic Innervation from PCs onto NBCs

Synaptic connections from 21 PCs onto NBCs were recorded throughout layers II–IV and five connections were reconstructed (Fig. 7*a*). PCs formed 3.4 ± 1.5 synapses onto NBCs, which is much fewer (~50%) than other types of interneurons within the same layers (unpublished observations). The average electrotonic distance of synaptic contacts (X = 0.041 ± 0.027) is also significantly lower compared to other interneurons (unpublished observations) and PCs (X = 0.083 ± 0.022, three connections, eight synapses; P < 0.05) within the same layers. This proximity of synaptic contacts is reflected in shorter synaptic delays (0.87 ± 0.28 ms; Table 3; Materials and Methods) compared with delays in the connections onto PCs in the same layer (1.52 ± 0.4 ms, n = 6; P < 0.01), indicating that NBCs will be excited nearly twice as rapidly as PCs. Interestingly, the monosynaptic delay between PCs is comparable to the net disynaptic delay via NBCs, indicating that once activated, PCs will receive virtually simultaneous excitation from PCs and inhibition from NBCs. In contrast to the distributed nature of synaptic contacts from NBCs onto PCs, synapses formed by PCs onto NBCs arose from the axonal main stem, the first and second PACs, and were more localized on the dendritic tree. Commonly two or more synapses originated from the same axonal segments (>75%; Table 3) and were clustered on only a few target cell dendrites (innervated dendritic fraction: 26%; Fig. 7*b*).

Synapses from PCs onto NBCs could be either facilitating (n = 5) or depressing (n = 16; Fig. 7*c*), depending on the intrinsic firing properties of the postsynaptic cell (see Table 3). Depressing synapses impinging onto NBCs display fast depression, most likely arising from high release probabilities (Table 3, Use parameter; see Materials and Methods). This effectively causes the synaptic response to shut down rapidly during a burst (Fig. 7*c*). The time constants of recovery from depression (D)

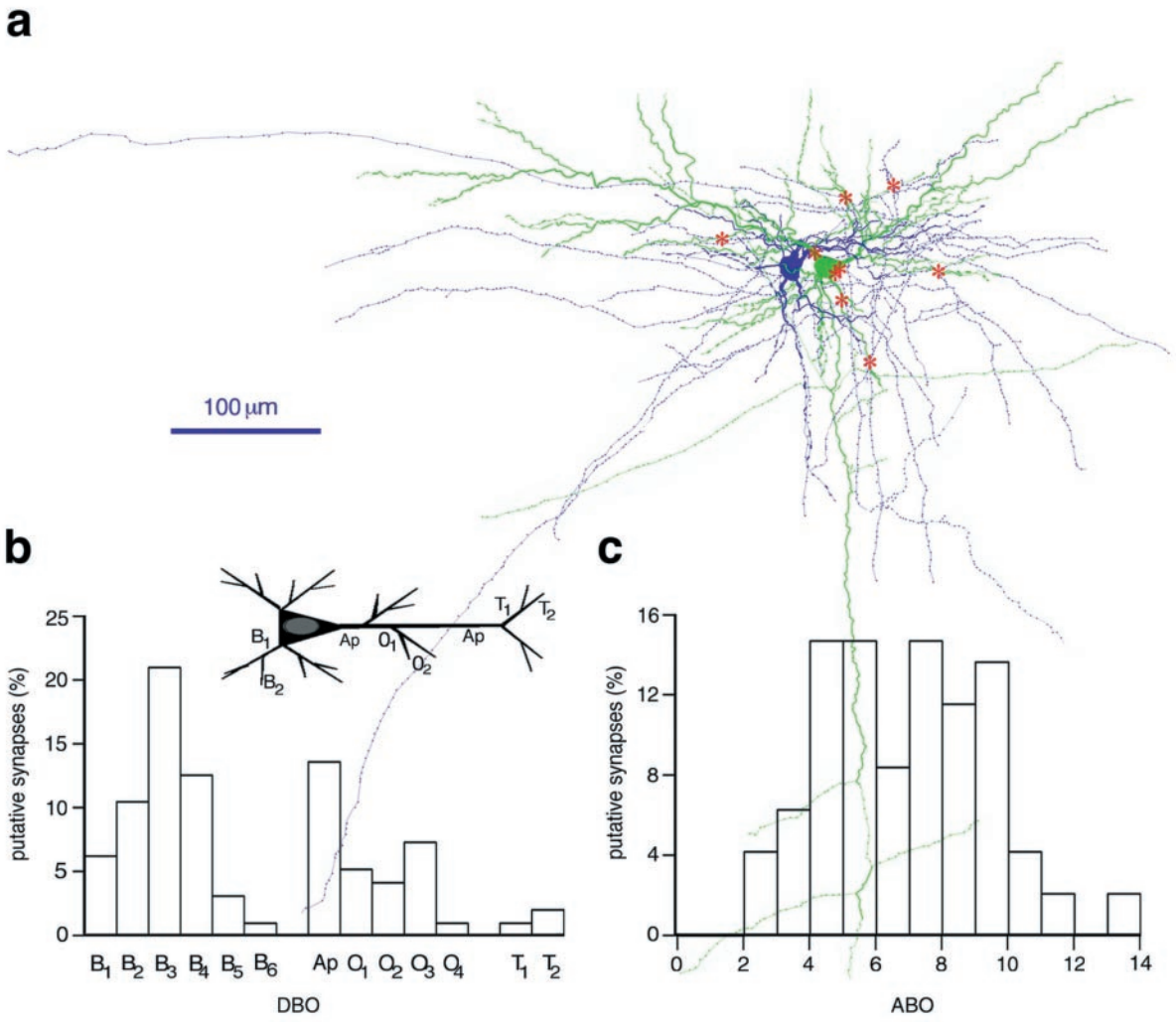

Figure 5. Anatomical properties of connections from NBCs to PCs. (*a*) Three-dimensional reconstruction of a NBC (blue) innervating a pyramidal cell (green) in layers II/III. Nine putative synapses (red asterisks) were formed in this connection (2 axo-somatic, 7 axo-dendritic). These putative axo-dendritic synapses were formed onto 3/4 dendritic trees (innervated dendritic fraction, 0.75) and originated from 5/7 primary axonal collaterals (innervating PAC fraction, 0.71). (*b*) Histogram of dendritic (postsynaptic) innervation pattern. Most of the putative synapses formed by NBCs were placed onto basal dendrites, particularly onto the second to fourth DBOs. Synapses impinging onto the apical dendrites were preferentially formed onto apical trunks ($P < 0.05$). Inset diagram illustrates the branch orders of different dendritic compartments of the postsynaptic PC. (*c*) Histogram of axonal (presynaptic) innervation pattern. Most synapses in connections from NBCs to PCs originate from fifth to tenth ABOs.

for synapses from PCs onto NBCs are however, much shorter (~230 ms; see Table 3) than those onto other PCs (~ 820 ms) (Markram *et al.*, 1998), allowing recruitment of NBCs up to considerably higher discharge rates. Facilitating synapses from a single PC were not strong enough to discharge NBCs, whereas other interneurons can be discharged from rest (Thomson and Deuchars, 1997; Markram *et al.*, 1998). This is probably due to the much lower number of synapses formed in connections onto NBCs. Regardless of the dynamics of the synapses employed, activity in several PCs are therefore required to recruit NBCs.

Properties of Synaptic Innervation between NBCs and Other Interneurons

Synaptic connections between interneurons were less frequently encountered than connections between interneurons and PCs (Gupta *et al*, 2000), and when connections were established, generally fewer putative synapses (8.92 ± 4.3; 13 reconstructions) were deployed than onto PCs. Presynaptic NBCs formed four putative synapses onto a bipolar interneuron and eight synapses onto a bitufted cell, respectively. Postsynaptic NBCs received 10 putative synapses from a neurogliaform cell (10/10 axo-dendritic) and six contacts from a bitufted cell (5/6 axo-dendritic), respectively. NBCs formed (F1, n = 2; F2, n = 6) and received (F1, n = 2; F2, n = 5) different types of GABAergic synapses (Fig. 7*d*). Despite the lower numbers of synaptic contacts in connections between interneurons, GABAergic transmission from a single presynaptic interneuron onto NBCs could effectively block spontaneous action potential discharge (Fig. 7*e*).

Discussion

We examined the morphological, physiological and molecular properties of basket cell-like interneurons in supragranular and granular layers of somatosensory cortex of rats. We found that a detailed quantification was demanded by the data in order to establish a concrete foundation for understanding interneuron diversity in general, and the diversity of BCs in particular. This analysis shows that BCs consist of three anatomically, physiologically and molecularly distinct subclasses (classical small and

Table 3
Quantitative analysis of synaptic connections between NBCs and PCs

	From NBC onto PCs	From PCs onto NBCs
Anatomical properties	(6 pairs, 93 synapses)	(5 pairs, 17 synapses)
No. of putative synapses	15.8 ± 4.1	3.4 ± 1.5
Innervated dendritic fraction[a]	0.78	0.26
Innervating PAC fraction[b]	0.83	–
Ratio of synapses sharing same axonal segments	0.25	0.76
Ratio of neighboring synapses within 10 μm	43%	41%
Dendritic synapse location : geometric distance (μm)	68.3 ± 13.1	54.6 ± 30.9
Dendritic synapse location : electotonic distance (λ)	0.063 ± 0.013	0.041 ± 0.027
Physiological properties	(11 pairs, all F2 type synapses)	(all depressing; $n = 7$; all CC)[c]
Unitary responses (VC, $n = 9$; CC, $n = 2$)[d]		
Failures (%)	0.74 ± 1.43	0 ± 0
CV of amplitudes	0.40 ± 0.09	0.32 ± 0.08
Current amplitude (pA)	26.4 ± 21.4	–
RT of synaptic currents (ms)	0.71 ± 0.23	–
DTC of synaptic currents (ms)	8.30 ± 2.67	–
Charge (nC)	0.24 ± 0.16	–
Conductance (nS)	1.03 ± 0.85	–
Mean latency (ms)	0.91 ± 0.24	0.87 ± 0.28
Synaptic dynamics (VC, $n = 4$)[e]		
Ase	343 ± 278 pA	3.98 ± 1.63 mV
Use	0.14 ± 0.05	0.72 ± 0.12
D (ms)	875 ± 285	227 ± 70
F (ms)	22 ± 5	13 ± 24
D:F ratio	44 ± 25	41 ± 40
G_{max} (nS)	10.16 ± 8.01	–
Synaptic mapping		
Electrophysiological subclass of NBC		
c-NAC	F3 (1/1)	facilitating (2/2)
d-NAC	F2 (15/15)	depressing (10/10)
c-AC	F2 (5/5)	facilitating (2/2)
b-AC	F2 (1/1)	facilitating (1/1)
d-AC; b-NAC	F2 (1/1); F2 (1/1)	–
b-STUT; c-STUT	F3 (1/1); F3 (1/1)	–
ND[f]	F2 (3/3); F3 (3/3)	depressing (6/6)

[a]Innervated dendritic fraction: the fraction of the dendritic trees of the postsynaptic cell receiving contacts from the presynaptic cell.

[b]Innervating PAC fraction: the fraction of the primary axonal collaterals (PAC) utilized to innervate the postsynaptic neuron.

[c]Physiological properties could not be reliably quantified due to synaptic rundown (Rozov *et al.*, 1998).

[d]VC = voltage clamp; CC = current clamp; RT = 20-80% rise time; DTC = decay time constant.

[e]Ase = absolute synaptic efficacy; Use = utilization of synaptic efficacy; D = time constant for recovery from synaptic depression; F = time constant for recovery from synaptic facilitation.

[f]ND denotes cases in which discharge properties were not obtained.

large BCs, and nest BCs) that are differentially distributed in cortical layers II–IV. Examination of synaptic input and output properties, suggests that multiple pyramidal cells are required to recruit NBCs, and that these interneurons powerfully inhibit a large fraction of the pyramidal cells in the supragranular and granular layers of the local cortical microcircuitry.

Defining Neocortical Basket Cells

The definition of neocortical BCs has been gradually refined since the original description by Ramon y Cajal (Ramon y Cajal, 1911). He noticed abundant, large multipolar cells with conspicuous long horizontal collaterals, which were considered the source of the salient terminal axonal arborizations around the somata and proximal dendrites of pyramidal neurons. These pericellular nests were only later shown to be formed by several of these cells described by Ramon y Cajal and called 'basket cells' (Marin-Padilla, 1969; Jones and Hendry, 1984; DeFelipe *et al.*, 1986; White, 1989). At the light microscopic level, short, bent axonal segments seemingly targeting neuronal somata have therefore been used as the general sign for classifying BCs (Ramon y Cajal, 1911; Jones and Hendry, 1984). EM studies confirmed high fractions of axo-somatic contacts (20–30%) in randomly sampled boutons of BCs (Somogyi *et al.*, 1983; Kisvarday *et al.*, 1985, 1987; Freund *et al.*, 1986). Basket cells are distinct from other types of interneurons in that they have the highest tendency to target somata. This criteria cannot be used strictly in the case of a small sample of synaptically coupled pairs, since any one basket cell does not form axo-somatic synapses onto every one of its target cells [see Results, and also (Kisvarday *et al.*, 1987; Tamas *et al.*, 1998)]. The distribution of synapses on the target neuron with respect to the soma should therefore be included in the definition of BCs: a strongly skewed distribution of steady-state electrotonic distances with >80% of synapses <0.1λ. Finally, the overall properties of axonal arbors provide reliable subjective and objective indicators of different interneuron types.

Soma sizes have also been considered when distinguishing small and large BCs (Jones and Hendry, 1984; Kisvarday, 1992), yet we did not find any significant differences. Furthermore, BCs are interneurons with highly diverse soma shapes as well as dendritic morphologies. Somata may have ovoid, triangular, inverted pyramidal or spindle shapes, and dendritic morphologies may be multipolar, bitufted or even bipolar. Soma size and shape as well as dendritic morphology are therefore unreliable for identifying interneurons in general, and subclasses of BCs in particular.

Three Subclasses of Basket Cells

LBCs and SBCs are easily classified as BCs at the light microscopic level based only on their soma targeting signs and overall axonal features. These classical BCs are also readily distinguished from each other according to their long horizontal axonal collaterals and short-range axonal plexus, respectively (Fairen *et al.*, 1984; Jones and Hendry, 1984; Kisvarday *et al.*, 1985). On the other hand, the smooth axonal collaterals of NBCs do not obviously target somata, leading to confusion as to whether such cells are *de facto* BCs. This could explain why numerous potential NBCs have remained unclassified (Jones, 1975; Jones and Hendry, 1984; Peters and Saint Marie, 1984; Lund and Lewis, 1993). In some cases, such cells seem to have been correctly identified as BCs, but then classified as SBCs because of some similarities in their soma–dendritic morphologies and local axonal plexus (DeFelipe and Fairen, 1982; Jones and Hendry, 1984; Peters and Saint Marie, 1984). SBCs and NBCs are, however, distinct in several respects. A quantitative analysis revealed several differences in dendritic and axonal features, and an even more striking demarcation at the molecular level. mRNA for VIP was found in all anatomically classified SBCs and in none of the NBCs or LBCs. Expression of mRNA for VIP or the protein itself is, therefore, a crucial factor in defining subclasses of BCs. Indeed, cells that seem to be BCs and that have been described as 'arcade cells' are VIP-positive and therefore most likely belong to the SBC subclass (Kawaguchi and Kubota 1996, 1997).

Expression patterns of mRNA for other neuropeptides seem less crucial for subclassifying BCs, although our data indicate that mRNA expression for NPY or SOM apparently precludes classification into SBCs or LBCs, respectively. These overall expression patterns therefore also indicate that the three subclasses of BC do not lie on a continuum (Cauli *et al.*, 1997; DeFelipe, 1993; Kawaguchi and Kubota, 1996, 1997; Porter *et al.*, 1998). Even if one considers the possibility of false negatives

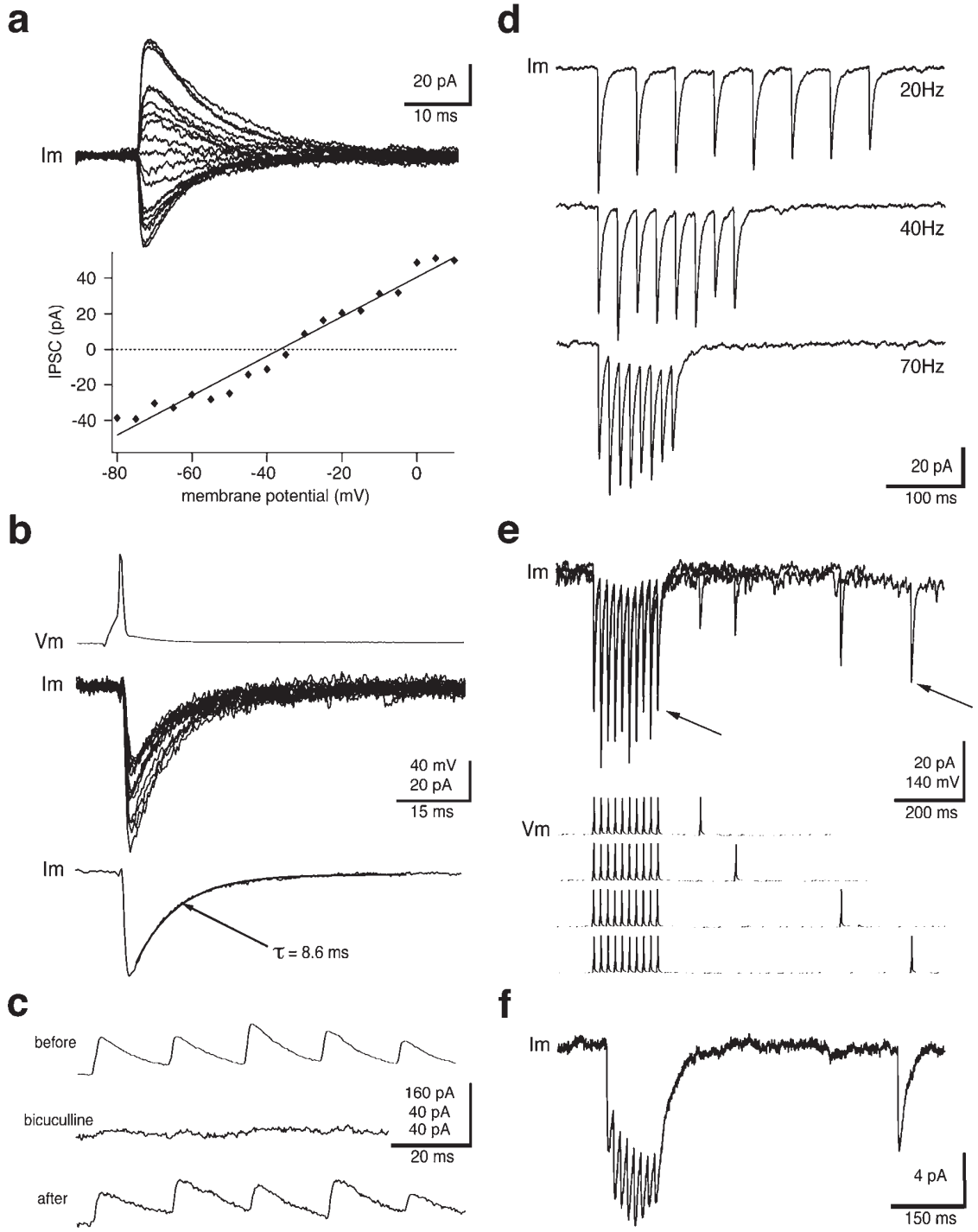

Figure 6. Physiological properties of connections from NBCs to PCs. (*a*) Synaptic currents reversing near −40 mV confirm GABAergic transmission. Each trace (upper panel) represents an average of 20 trials. Lower panel plots peak current amplitudes against holding potential for traces shown in upper panel (not corrected for liquid junction potential of ~9 mV). (*b*) Consecutive trials of unitary current responses in postsynaptic pyramidal neuron (middle panel, 15 traces overlaid) to action potentials in the presynaptic NBC (upper trace). Lower trace represents average of traces shown in middle panel. Monoexponential fit shows characteristic slow decay of GABAergic currents. (*c*) Synaptic current responses in a pyramidal cell (V_{hold} = 0 mV) to high frequency stimulation of presynaptic NBC (50 Hz train, 30 APs; only the first five PSCs shown) were completely and reversibly blocked by bath application of bicuculline (10 μM). (*d*) Dynamic properties of synaptic transmission from NBCs to PCs. Note the seeming absence of short duration facilitation at low frequencies (upper panel, 20 Hz), which is gradually unmasked at higher frequencies (middle 40 Hz, lower trace 70 Hz). (*e*) F2-type GABAergic synaptic responses in postsynaptic PC (upper panel) to stimulation of presynaptic NBC (AP trains, lower panel). Note the short lasting facilitation of synaptic responses within high frequency trains (50 Hz; see also *d*) and long lasting depression of responses following the train. RTRs tested up to 700 ms following high frequency trains were depressed compared with even the last response within the train (arrows). (*f*) F3-type GABAergic synapses from NBC to PC. Note that the synapse has fully recovered by the time the RTR is delivered (500 ms after train).

or ultra-low mRNA levels, one would hardly expect mRNA profiles to follow perfectly an independent anatomical classification. The mRNA profiles are also used strictly for the purpose of molecular classification and not to infer functional significance, because the relationship between mRNA levels and protein expression is complex.

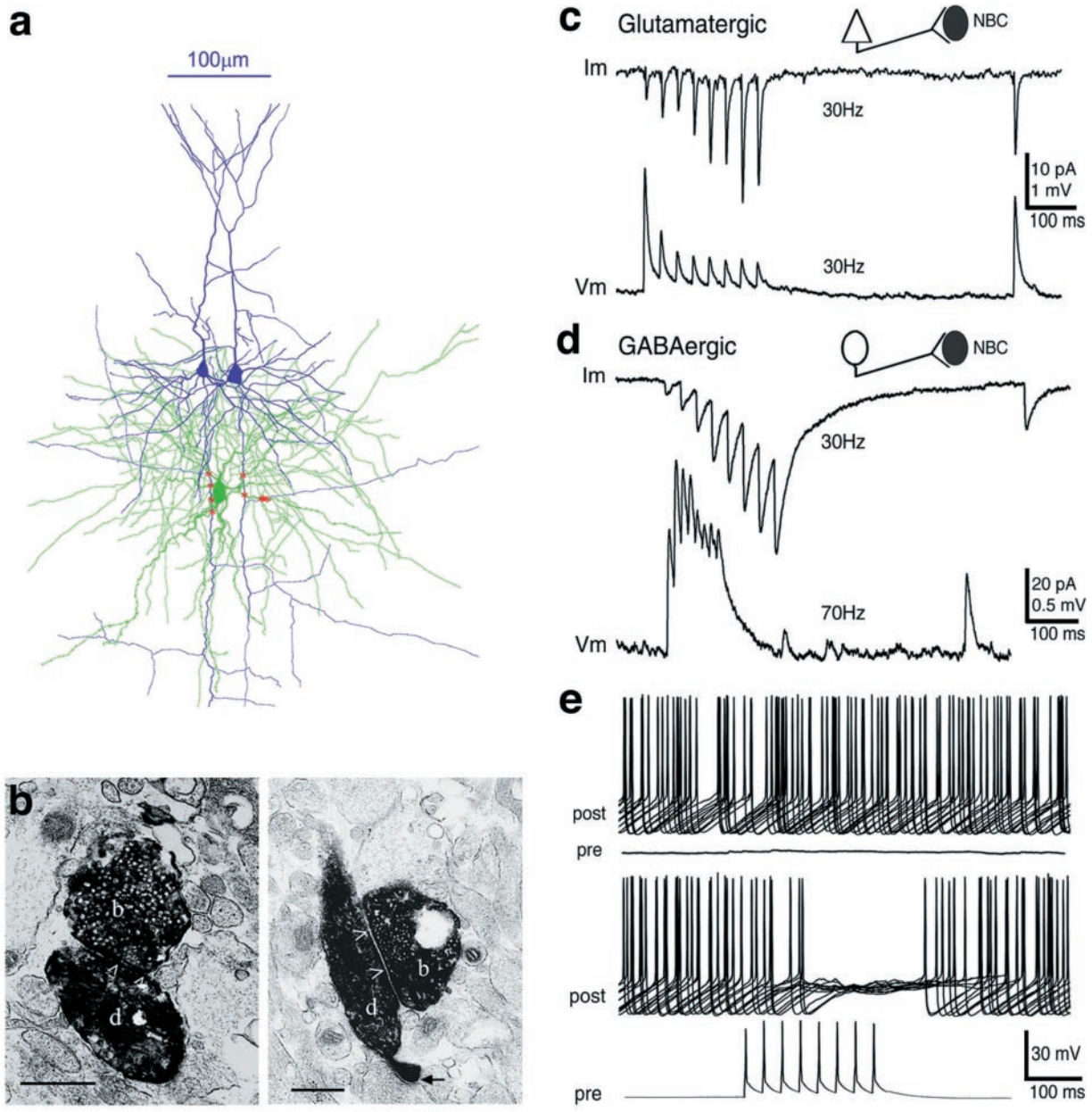

Figure 7. Postsynaptic NBCs receive different types of glutamatergic and GABAergic inputs. (*a*) Three-dimensional computer reconstruction of an NBC (green) receiving convergent glutamatergic inputs from two presynaptic PCs (blue). The left PC formed four putative synapses (red asterisks) with the boutons located on its main axonal stem; the right PC formed five putative synapses onto a NBC (two from the main axonal stem; three closely located to each other from first primary axonal collateral). (*b*) Electron micrographs of axo-dendritic synapses formed from a PC onto a NBC. Between the rigid pre- and postsynaptic membranes, the synaptic clefts at the sites of the synaptic junctions are delimited by arrowheads. An additional synapse formed by an unlabeled bouton onto the same dendritic structure can be seen on right panel (arrow). The synaptic cleft in the left panel is partly obscured by the suboptimal goniometric angle; scale bar = 0.5 μm. (*c*) Glutamatergic inputs onto NBCs can be either classically facilitating (upper, current trace) or depressing (lower, voltage trace). Inset scheme: open triangle symbolizes presynaptic PC, closed ellipsoid symbolizes postsynaptic NBC. (*d*) GABAergic inputs onto NBCs display either F1- (upper, current trace) or F2- type (lower, voltage trace) synaptic dynamics. Note the slower decays of GABAergic synaptic currents compared with glutamatergic currents. Inset scheme: the open ellipsoid symbolizes a presynaptic interneuron, the closed ellipsoid symbolizes the postsynaptic NBC. (*e*) Interneurons can effectively prevent spontaneous action potential (AP) discharge in NBCs. Spontaneous spiking of postsynaptic NBC (upper voltage traces, post Vm) in the absence (flat voltage trace, pre Vm) and presence of stimulation of the presynaptic interneuron (lowermost voltage trace, pre Vm). Note the delay of the AP blockade due to the F1-dynamics of the synapses impinging onto the postsynaptic NBC.

In the current study, labeled pairs of presynaptic NBCs innervating postsynaptic targets revealed frequent putative axo-somatic synapses formed by smooth axonal collaterals, which was less frequent than the 20–30% required in the traditional definition, but too often compared to other clearly dendritic targeting cells. Indeed, like other BCs, >80% of synapses were electrotonically located within 0.1λ of somata. NBCs typically formed axo-somatic autapses (unpublished observations), which is also characteristic of BCs (Tamas *et al.*, 1997b). Finally, EM of randomly selected boutons verified a high fraction of axo-somatic synapses formed by NBCs. These interneurons are therefore BCs, but because of their distinctive axonal and dendritic features and molecular expression patterns, they constitute a separate subclass of BCs.

This study thus shows that it is justified to apply the following subjective anatomical guidelines to distinguish the three subclasses of BCs.

- *Large Basket Cells* are interneurons with somata that give rise to several aspiny, beaded dendrites and have axons with a low density of boutons that characteristically generate conspicuous long-range horizontal collaterals traversing multiple columns. The axon usually arises from the pial aspect and produces a characteristic *sparse* plexus of axonal collaterals made up of a few long, straight branches, as well as some vertically and horizontally projecting collaterals that may cross all layers and columns, respectively.
- *Small Basket Cells* are interneurons with somata that give rise to 2–4 aspiny and beaded dendrites and a *dense* local plexus of highly varicose axons. This characteristic plexus is formed by frequent short, curvy axonal branches, densely studded with boutons, which remain in the same column and layer. Occasionally SBCs may generate a few far-reaching collaterals projecting across layers and columns.
- *Nest Basket Cell* somata give rise to nearly aspiny, radially projecting beaded dendrites and a *sparse to dense* local axonal plexus around somata, and may generate long horizontal axons. This characteristic plexus is formed by infrequent long, smoothly bending axonal branches, sparsely studded with boutons, which mainly remain in the same column and layer. NBCs also exhibit a characteristically simple dendritic arbor with few short, infrequently branch- ing dendrites. NBCs may appear highly heterogeneous upon subjective analysis, but a quantitative analysis yields much greater uniformity of multiple morphological features.

This classification can be validated by quantitative morphometric analyses and confirmed by their molecular profiles. The study was, however, carried out at a stage of rapid neocortical development where properties such as synapse numbers and structure of connectivity are changing rapidly and extrapolations to fully matured neocortex should be made with caution. It is unlikely that the NBC is merely an intermediate cell type between LBCs and SBCs that is present only transiently during development since many of the anatomical features and molecular profiles of NBCs as well as LBCs and SBCs are consistent with numerous reports from adult animals in different areas and across several species (Ramon y Cajal, 1911; Jones, 1975; Fairen *et al.*, 1984; Jones and Hendry, 1984; Peters and Saint Marie, 1984; Kisvarday *et al.*, 1985; DeFelipe, 1993; Lund and Lewis, 1993; Cauli *et al.*, 1997; Kawaguchi and Kubota, 1996, 1997; Thomson and Deuchars, 1997; Porter *et al.*, 1998). This study therefore does not describe a novel cell type, but provides the subjective and objective features of variants of BCs that have been observed by many authors. The current study suggests that the basket cell diversity can be understood in terms of three major subclasses.

The three subclasses of BCs are differentially distributed in layers II/III and IV. NBCs were the most common BC subclass encountered in layers II/III of somatosensory cortex in the present study (73%), and constitute a major fraction in layer IV (34%). Only a small fraction of the BCs in layer II/III were found to be SBCs. These values are little affected by a pre-selection bias because one cannot reliably distinguish any of these subclasses (in fact any type of interneuron, including BCs, bitufted, double bouquet and chandelier cells) at the infrared differential contrast level, where only the soma and part of the dendrites are visible — even after full reconstruction, it is largely the axonal arborization that distinguishes the different interneurons. We have also recorded NBCs in layer V (unpublished observations). A recent report on supragranular interneurons in rat visual cortex also mentions this cell type (Dantzker and Callaway, 2000), indicating that NBCs are not confined to the somatosensory area. Furthermore, numerous atypical BCs, some of which were broadly defined as 'medium arbor' or 'local plexus' neurons, have been encountered in all layers in different cortical areas of several species (Fairen *et al.*, 1984; Peters and Saint Marie, 1984; White, 1989; Lund and Lewis, 1993), suggesting that NBCs are probably ubiquitous.

A particular type of basket cell, known as clutch cell, seems to be the major type of basket cell in layer IV of visual cortices in cats and monkeys (Kisvarday, 1992). These cells, originally suggested as a subclass of SBC, owe their name to their distinctive 'claw-like' terminal axonal configurations (Kisvarday *et al.*, 1985). This particular axonal configuration was not prominent in somatosensory cortex of juvenile rats. However, some morphological features of clutch cells are consistent with those of SBCs in this study (e.g. short axonal segments, high bouton density and frequent branching) (Kisvarday *et al.*, 1985), further suggesting that clutch cells may be a subclass of SBC.

Impact of NBCs in the Neocortex

A large number of synapses, highly distributed on the axonal arbor of the presynaptic NBC and on the somato-dendritic domain of the postsynaptic PC, provide the anatomical basis for powerful and reliable signal transmission. The significant fraction of axo-dendritic synapses onto PCs may enable NBCs to influence synaptic integration and regulate AP-generation and propagation within dendrites, while the (peri-)somatic inhibition could control the gain of summated potentials and block AP-generation (Cobb *et al.*, 1995; Miles *et al.*, 1996; Larkum *et al.*, 1999). Indeed, a single NBC can delay as well as block spontaneous AP-discharges in postsynaptic PCs (n = 2, unpublished observations). Rough estimates indicate that each NBC targets 150–170 PCs and 25–35 interneurons within layers II/III and within a 300 μm diameter (mean slice error of ~25%, 1.1 synapses/bouton, 70% intracolumnar synapses, ~16 synapses/PC, ~6 synapses/interneuron, 25% interneurons), indicating that each NBC can powerfully inhibit ~10% of the PCs within the layer and within this lateral extent (~1500 PCs) (Ren *et al.*, 1992). Basket cells constitute ~50% of the interneurons in layer II/III (unpublished data), of which 73% are NBCs, indicating that these provide a major fraction of the inhibition in this layer. While the impact on individual PCs is potentially powerful, the low density of boutons and similar numbers of synapses deployed in connections onto PCs compared with SBCs indicates that each NBC innervates fewer PCs in the local microcircuit compared to a single SBC.

NBCs are often reciprocally connected to neighboring PCs (11/32 cases), indicating that a significant fraction of inhibition is applied to those PCs locally involved in exciting them. These circuit principles could enable NBCs to synchronize target-cell activity (Cobb *et al.*, 1995), potentially leading to network oscillations (Buzsaki and Chrobak, 1995; McBain and Fisahn, 2001). The connectivity between NBCs and other types of interneurons could also favor network synchrony (Buzsaki and Chrobak, 1995; Tamas *et al.*, 1998), as could electrical junctions (Galarreta and Hestrin, 1999; Gibson *et al.*, 1999).

The inhibitory impact of NBCs is temporally complex because electrophysiological subclasses of NBCs employ synapses with different temporal dynamics to inhibit PCs, indicating that the convergence of different subclasses of NBCs could result in a

range of different effects (see Fig. 6). Interneurons characteristically exert the same temporal impact onto groups of targets (Gupta *et al.*, 2000), indicating that while the NBC population as a whole exerts a temporally heterogenous effect, a single NBC exerts a temporally homogeneous effect onto groups of target cells. It is important to note that many dynamic features are known to change with development, thus the precise synaptic parameters or the large spectrum of electrophysiological patterns may not be generally extrapolated to adult animals (Bolshakov and Siegelbaum, 1995; Reyes and Sakmann, 1999).

Recruitment of NBCs by Pyramidal Cells

Glutamatergic synapses formed onto neocortical interneurons in different areas and species are known to display either frequency-dependent facilitation or depression. Moreover, the same pyramidal neuron can form different types of synapses onto different target cells (Markram *et al.*, 1998; Reyes *et al.*, 1998; Wang *et al.*, 1999). Synapses formed onto sparsely spiny, bitufted interneurons typically display facilitation (Thomson and Deuchars, 1997; Markram *et al.*, 1998; Reyes *et al.*, 1998; Wang *et al.*, 1999), whereas those formed onto aspiny, multipolar interneurons (presumed LBCs) typically display depression (Buhl *et al.*, 1997; Thomson and Deuchars, 1997; Galarreta and Hestrin, 1998; Reyes *et al.*, 1998). This has led to the notion, that anatomically distinct interneuron types exclusively receive either facilitating or depressing glutamatergic synapses (Reyes *et al.*, 1998; Zilberter *et al.*, 1999). Our data suggest that it is not sufficient to consider only the broad anatomical classification since LBCs and NBCs can receive either facilitating or depressing synapses due to the heterogeneity (as measured in terms of electrophysiological properties) within these classes.

We estimate that a single NBC in layers II/III receives inputs from 180–220 presynaptic PCs and 15–30 presynaptic interneurons which is similar to the numbers estimated for LBCs and SBCs (analysis not shown). The number of synapses employed by PCs to recruit NBCs is much lower than for other interneurons (unpublished data) and also nearly five times lower than the number used by NBCs to innervate PCs. The few synapses in these glutamatergic connections suggest that more PCs are required to recruit NBCs than most other interneurons, suggesting that these are 'high threshold interneurons' from the perspective of the PC population. Indeed, unlike inputs onto most other interneurons, a single PC could not discharge an NBC even when strongly facilitating synapses were present. While the general activity level may be the highest for neighboring PCs to recruit NBCs, the axonal and dendritic proximity underlie very short latencies and ensure that NBCs are recruited with very high temporal precision. Indeed, NBCs are excited almost twice as rapidly as neighboring PCs, and the disynaptic delay from PC to NBC to PC is essentially as fast as the monosynaptic excitation (PC to PC). The outcome of this temporal coincidence of excitation and inhibition will, however, be more elaborate, since the temporal dynamics of the different synapses involved can differ strikingly.

Different electrophysiological subtypes of NBCs targeted by the same presynaptic pool of PCs are differentially recruited owing to the underlying differences in the dynamic properties of the impinging synapses (Markram *et al.*, 1998). These synaptic properties could, however, be different in adult animals, since the dynamics of glutamatergic synaptic transmission are subject to developmental changes (Reyes and Sakmann, 1999), and electrophysiological properties may also change. Nevertheless, at this age, different subtypes of NBCs respond differently to activity in the PCs. NBCs receiving facilitating synapses generally respond more to the tonic (rate) component of the population activity of presynaptic PCs, whereas NBC subclasses receiving depressing synapses generally respond more to the phasic (changes) component of the PC-population activity (Markram *et al.*, 1998). The complex dynamics of synapses deployed onto different electrophysiological subtypes of NBCs therefore provide a potential biophysical basis for multiple dynamic thresholds for recruiting different subclasses of NBCs.

Notes

We thank Professors E. White, M. Gutnick, Y. Dudai and G. Silberberg for comments on the manuscript, Prof. P. Somogyi for the guidance in EM work, and Drs G. Getz and N. Kalisman for the assistance in the clustering analysis. This study was supported by grants from the Office of Naval Research, the Human Frontier Science Program, the Minerva Foundation, and the Shane and Blum Foundations. H.M. holds the Helen and Stanley Diller Chair in Neurobiology and is supported by the Dolfi and Lola Ebner Research Award in Biomedicine. A.G. is a Minerva Fellow.

Address correspondence to Henry Markram, Department of Neurobiology, Weizmann Institute of Science, 76100 Rehovot, Israel. Email: henry.markram@weizmann.ac.il.

References

Aranda-Abreu GE, Behar L, Chung S, Furneaux H, Ginzburg I (1999) Embryonic lethal abnormal vision-like RNA-binding proteins regulate neurite outgrowth and tau expression in PC12 cells. J Neurosci. 19: 6907–6917.

Berman NJ, Douglas RJ, Martin KA. (1992) GABA-mediated inhibition in the neural networks of visual cortex. Prog Brain Res 90:443–476.

Bolshakov VY, Siegelbaum SA (1995) Regulation of hippocampal transmitter release during development and long-term potentiation. Science 269:1730–1734.

Buhl EH, Tamas G, Szilagyi T, Stricker C, Paulsen O, Somogyi P (1997) Effect, number and location of synapses made by single pyramidal cells onto aspiny interneurons of cat visual cortex. J Physiol (Lond) 500: 689–713.

Buzsaki G, Chrobak JJ (1995) Temporal structure in spatially organized neuronal ensembles: a role for interneuronal networks. Curr Opin Neurobiol 5:504–510.

Cauli B, Audinat E, Lambolez B, Angulo MC, Ropert N, Tsuzuki K, Hestrin S, Rossier J (1997) Molecular and physiological diversity of cortical nonpyramidal cells. J Neurosci 17:3894–3906.

Cobb SR, Buhl EH, Halasy K, Paulsen O, Somogyi P (1995) Synchronization of neuronal activity in hippocampus by individual GABAergic interneurons. Nature 378:75–78.

Connors BW, Gutnick MJ (1990) Intrinsic firing patterns of diverse neocortical neurons. Trends Neurosci 13:99–104.

Dantzker JL, Callaway EM (2000) Laminar sources of synaptic input to cortical inhibitory interneurons and pyramidal neurons. Nat Neurosci 3:701–707.

DeFelipe J (1993) Neocortical neuronal diversity: chemical heterogeneity revealed by colocalization studies of classic neurotransmitters, neuropeptides, calcium binding proteins, and cell surface molecules. Cereb Cortex 3:273–289.

DeFelipe J, Fairen A (1982) A type of basket cell in superficial layers of the cat visual cortex. A Golgi-electron microscope study. Brain Res 244:9–16.

DeFelipe J, Hendry SH, Jones EG (1986) A correlative electron microscopic study of basket cells and large GABAergic neurons in the monkey sensory-motor cortex. Neuroscience 17:991–1009.

Fairen A, DeFelipe J, Regidor J (1984) Nonpyramidal neurons: general account. In: Cerebral cortex: cellular components of the cerebral cortex (Peters A, Jones EG, eds), pp. 201–245. New York: Plenum Press.

Feldman ML, Peters A (1978) The for.m.s. of non-pyramidal neurons in the visual cortex of the rat. J Comp Neurol 179:761–793.

Freund TF, Magloczky Z, Soltesz I, Somogyi P (1986) Synaptic connections, axonal and dendritic patterns of neurons immunoreactive for cholecystokinin in the visual cortex of the cat. Neuroscience 19: 1133–1159.

Fukunaga K (1990) Introduction to statistical pattern recognition. San Diego, CA: Academic Press.

Galarreta M, Hestrin S (1997) Properties of GABA-A receptors underlying inhibitory synaptic currents in neocortical pyramidal neurons. J Neurosci 17:7220–7227.
Galarreta M, Hestrin S (1998) Frequency-dependent synaptic depression and the balance of excitation and inhibition in the neocortex. Nat Neurosci 1:587–594.
Galarreta M, Hestrin S (1999) A network of fast-spiking cells in the neocortex connected by electrical synapses. Nature 402:72–75.
Gibson JR, Beierlein M, Connors BW (1999) Two networks of electrically coupled inhibitory neurons in neocortex. Nature 402:75–79.
Gupta A, Wang Y, Markram H (2000) Organizing principles for a diversity of GABAergic interneurons and synapses in the neocortex. Science 287:273–278.
Han ZS, Buhl EH, Lorinczi Z, Somogyi P (1993) A high degree of spatial selectivity in the axonal and dendritic domains of physiologically identified local-circuit neurons in the dentate gyrus of the rat hippocampus. Eur J Neurosci 5:395–410.
Hornung JP, Garey LJ (1981) The thalamic projection to cat visual cortex: ultrastructure of neurons identified by Golgi impregnation or retrograde horseradish peroxidase transport. Neuroscience 6:1053–1068.
Houser CR, Vaughn JE, Hendry SHC, Jones EG, Peters A (1984) GABA neurons in the cerebral cortex. In: Cerebral cortex: functional properties of cortical cells (Peters A, Jones EG, eds), pp. 63–87. New York: Plenum Press.
Jones EG (1975) Varieties and distribution of non-pyramidal cells in the somatic sensory cortex of the squirrel monkey. J Comp Neurol 160:205–267.
Jones EG, Hendry SHC (1984) Basket cells. In: Cerebral cortex: cellular components of the cerebral cortex (Peters A, Jones EG, eds), pp. 309–334. New York: Plenum Press.
Kawaguchi Y, Kubota Y (1996) Physiological and morphological identification of somatostatin- or vasoactive intestinal polypeptide-containing cells among GABAergic cell subtypes in rat frontal cortex. J Neurosci 16:2701–2715.
Kawaguchi Y, Kubota Y (1997) GABAergic cell subtypes and their synaptic connections in rat frontal cortex. Cereb Cortex 7:476–486.
Kawaguchi Y, Kubota Y (1998) Neurochemical features and synaptic connections of large physiologically identified GABAergic cells in the rat frontal cortex. Neuroscience 85:677–701.
Kisvarday ZF (1992) GABAergic networks of basket cells in the visual cortex. Prog Brain Res 90:385–405.
Kisvarday ZF, Martin KA, Whitteridge D, Somogyi P (1985) Synaptic connections of intracellularly filled clutch cells: a type of small basket cell in the visual cortex of the cat. J Comp Neurol 241:111–137.
Kisvarday ZF, Martin KA, Friedlander MJ, Somogyi P (1987) Evidence for interlaminar inhibitory circuits in the striate cortex of the cat. J Comp Neurol 260:1–19.
Krimer LS, Goldman-Rakic PS (2001) Prefrontal microcircuits: membrane properties and excitatory input of local, medium, and wide arbor interneurons. J Neurosci. 21:3788–3796.
Kubota Y, Kawaguchi Y. (1997) Two distinct subgroups of cholecystokinin-immunoreactive cortical interneurons. Brain Res 752:175–183.
Lambolez B, Audinat E, Bochet P, Crepel F, Rossier J (1992) AMPA receptor subunit expressed by single Purkinje cell. Neuron 9: 247–258.
Larkum ME, Zhu JJ, Sakmann B (1999) A new cellular mechanism for coupling inputs arriving at different cortical layers. Nature 398: 338–341.
Lund JS, Lewis DA (1993) Local circuit neurons of developing and mature macaque prefrontal cortex: Golgi and immunocytochemical characteristics. J Comp Neurol 328:282–312.
Marin-Padilla M (1969) Origin of the pericellular baskets of the pyramidal cells of the human motor cortex. Brain Res 14:633–646.
Markram H, Lubke J, Frotscher M, Roth A, Sakmann B (1997) Physiology and anatomy of synaptic connections between thick tufted pyramidal neurons in the developing rat neocortex. J Physiol (Lond) 500: 409–440.
Markram H, Wang Y, Tsodyks M (1998) Differential signaling via the same axon of neocortical pyramidal neurons. Proc Natl Acad Sci USA 95:5323–5328.
Martin KA, Somogyi P, Whitteridge D (1983) Physiological and morphological properties of identified basket cells in the cat's visual cortex. Exp Brain Res 50:193–200.
McBain CJ, Fisahn A (2001) Interneurons unbound. Nat Rev Neurosci 2:11–23.
Miles R, Toth K, Gulyas AI, Hajos N, Freund TF (1996) Differences between somatic and dendritic inhibition in the hippocampus. Neuron 16:815–823.
Peters A (1984) Numbers of neurons and synapses in primary visual cortex. In: Cerebral cortex: cellular components of the cerebral cortex (Peters A and Jones EG, eds), pp. 267–292. New York: Plenum Press.
Peters A, Harriman KM (1992) Different kinds of axon terminals forming symmetric synapses with the cell bodies and initial axon segments of layer II/III pyramidal cells. III. Origins and frequency of occurrence of the terminals. J Neurocytol 21:679–692.
Peters A, Saint Marie RL (1984) Smooth and sparsely spinous non-pyramidal cells forming local axonal plexuses. In Cerebral cortex: cellular components of the cerebral cortex (Peters A, Jones EG, eds), pp. 419–442. New York: Plenum Press.
Peters A, Palay SL, Webster HD (1991) The fine structure of the nervous system: neurons and their supporting cells. New York: Oxford University Press.
Porter JT, Cauli B, Staiger JF, Lambolez B, Rossier J, Audinat E (1998) Properties of bipolar VIPergic interneurons and their excitation by pyramidal neurons in the rat neocortex. Eur J Neuroscience 12:3617–3628.
Ramon y Cajal S (1911) Histologie de systeme nerveux de l Homme et des vertebres tomme II. Paris: Maloine.
Ren JQ, Aika Y, Heizmann CW, Kosaka T (1992) Quantitative analysis of neurons and glial cells in the rat somatosensory cortex, with special reference to GABAergic neurons and parvalbumin-containing neurons. Exp Brain Res 92:1–14.
Reyes A, Lujan R, Rozov A, Burnashev N, Somogyi P, Sakmann B (1998) Target-cell-specific facilitation and depression in neocortical circuits. Nat Neurosci 1:279–285.
Reyes A, Sakmann B (1999) Developmental switch in the short-term modification of unitary EPSPs evoked in layer 2/3 and layer 5 pyramidal neurons of rat neocortex. J Neurosci 19:3827–3835.
Rozov A, Zilberter Y, Wollmuth LP, Burnashev N (1998) Facilitation of currents through rat Ca^{2+}-permeable AMPA receptor channels by activity-dependent relief from polyamine block. J Physiol (Lond) 511:361–377.
Sholl DA (1956) The organization of the cerebral cortex. London: Methuen.
Somogyi P, Soltesz I (1986) Immunogold demonstration of GABA in synaptic terminals of intracellularly recorded, horseradish peroxidase-filled basket cells and clutch cells in the cat's visual cortex. Neuroscience 19:1051–1065.
Somogyi P, Kisvarday ZF, Martin KA, Whitteridge D (1983) Synaptic connections of morphologically identified and physiologically characterized large basket cells in the striate cortex of cat. Neuroscience 10:261–294.
Tamas G, Buhl EH, Somogyi P (1997a) Fast IPSPs elicited via multiple synaptic release sites by different types of GABAergic neuron in the cat visual cortex. J Physiol (Lond) 500:715–738.
Tamas G, Buhl EH, Somogyi P (1997b) Massive autaptic self-innervation of GABAergic neurons in cat visual cortex. J Neurosci 17:6352–6364.
Tamas G, Somogyi P, Buhl EH (1998) Differentially interconnected networks of GABAergic interneurons in the visual cortex of the cat. J Neurosci 18:4255–4270.
Thomson AM, Deuchars J (1997) Synaptic interactions in neocortical local circuits: dual intracellular recordings *in vitro*. Cereb Cortex 7:510–522.
Thomson AM, West DC, Hahn J, Deuchars J (1996) Single axon IPSPs elicited in pyramidal cells by three classes of interneurones in slices of rat neocortex. J Physiol (Lond) 496:81–102.
Valverde F (1971) Short axon neuronal subsystems in the visual cortex of the monkey. Int J Neurosci 1:181–197.
Wang Y, Gupta A, Markram H (1999) Anatomical and functional differentiation of glutamatergic synaptic innervation in the neocortex. J Physiol (Paris) 93:305–317.
White E (1989) Cortical circuits: synaptic organization of the cerebral cortex; structure, function, and theory. Boston, MA: Birkhauser Verlag.
Zilberter Y, Kaiser KM, Sakmann B (1999) Dendritic GABA release depresses excitatory transmission between layer 2/3 pyramidal and bitufted neurons in rat neocortex. Neuron 24:979–988.